91602
new 82-10

COMPLIMENTARY COPY
Please Credit Ontario Hydro Research if
Reproduced in Whole or in Part

ontario hydro
research division

TEST PROGRAM OF THE PROTOTYPE OF THE TWPP CONTAINER PART 1- HYDROSTATIC TESTS

Report No 84-293-K

B. Teper
Engineer
Applied Structural and Solid Mechanics Section
Mechanical Research Department

ABSTRACT

The TWPP (Thin-Wall, Particulate-Packed) container was designed for immobilization and disposal of used fuel bundles from the CANDU Nuclear Power Stations. A full scale prototype of this container has been built to demonstrate its structural performance under postulated sets of loads. The performance was tested using the fully assembled container with both optimal particulate packing and under simulated void conditions. The container was subjected to six separate pressure loading conditions without failure of its pressure boundary. Only small, compressive plastic deformations occurred throughout the vessel, as predicted by the preliminary stress analysis. This is Part 1 of the four part comprehensive report, detailing the testing and evaluation of the prototype of the TWPP container. In part 1, the activities leading to and including the hydrostatic test program are described.

job	file	date	report no.
740621-111-461	825.94	December 21, 1984	84-293-K

91602
new 82-10

ontario hydro
research division

EXECUTIVE SUMMARY

TEST PROGRAM OF THE PROTOTYPE OF THE TWPP CONTAINER PART 1- HYDROSTATIC TESTS

B. Teper

The thin-wall, particulate-packed container concept was designed for immobilization and disposal of used fuel bundles from the CANDU Nuclear Power Stations. A prototype container was designed and procured by the Mechanical Design Department.

Research Division examined the prototype and found significant weld and other flaws. In spite of these flaws, all tests were completed successfully.

During assembly of the container, good fluidity and ease of packing of the proposed particulate were demonstrated. Void free packing was achieved without significant difficulty. The hydrostatic test demonstrated an adequate strength of the vessel and particulate. Small, compressive plastic deformations occurred throughout the vessel, as predicted by the preliminary stress analysis. Even artificially induced voids in the particulate, totalling 1.85 L did not cause the prototype to fail, although more significant, localized strains and instabilities were observed. Stresses in the vessel due to handling are negligible.

The thin-wall, particulate-packed container represents a structurally viable option for disposal of used fuel from CANDU reactors.

The following report is Part 1 of a comprehensive report detailing the studies performed on and associated with the prototype of the TWPP container. Part 1 deals with activities leading to and including the hydrostatic test program.

job	file	date	report no.
740621-111-461	825.94	December 21, 1984	84-293-K

TABLE OF CONTENTS

	Page
NOMENCLATURE	ii
NOTATION	iii
LAYOUT OF REPORT	iv
1.0 INTRODUCTION	1
2.0 DESCRIPTION OF PROTOTYPE	3
3.0 ASSEMBLY OF CONTAINER	3
3.1 Shaker Table	3
3.2 Ontario Hydro Container	4
3.3 Closure	5
4.0 SHIPMENT OF CONTAINER TO WNRE	6
5.0 INSTRUMENTATION OF CONTAINER	6
6.0 HYDROSTATIC TEST PROGRAM	7
6.1 Test Facility	7
6.2 Preliminary Tests	7
6.3 First-Stage Test	8
6.4 Second-Stage Test	9
6.5 Full Pressure and Temperature Test	10
6.6 Long Term Test	10
6.7 Centre Void Test	10
6.8 Side Void Test	11
7.0 COMPARISON OF TEST RESULTS WITH PRELIMINARY STRESS ANALYSIS	11
8.0 CONCLUSIONS	12
9.0 ACKNOWLEDGEMENTS	13
REFERENCES	14
APPENDIX A TABLES	15
APPENDIX B FIGURES	20
APPENDIX C HYDROSTATIC TEST RESULTS	50
APPENDIX D SEAL FAILURE	68
APPENDIX E PARTICULATE STIFFNESS CONSIDERATION	74
DISTRIBUTION	last page

NOMENCLATURE

Bristol Container	- synonymous with particulate-packed, structurally-supported container built by Bristol Aerospace Limited
Container	- a receptacle used for the encapsulation of nuclear fuel waste prior to disposal
Disposal Facility	- a facility used to emplace or discharge waste materials with no intention of retrieval (for example, an underground disposal vault and its supporting facilities)
Disposal System	- a disposal facility and the transportation facilities needed to bring nuclear fuel wastes from the interim storage sites
Ontario Hydro Container	- synonymous with thin-wall, particulate-packed container, designed and built by Ontario Hydro
OHRD	- Ontario Hydro Research Division
TWPP	- Thin-Wall, Particulate-Packed
Used Fuel	- fuel extracted from a reactor at an end of its useful cycle, and containing significant amounts of plutonium and other fission products in excess of 0.25 mCi

NOTATION

D - plate constant $D = Et^3/12(1-D^2) = 9.1 \times 10^5$ mmN

E - modulus of elasticity of a metal

E_c - effective stiffness of cylindrical shell

E_f - effective stiffness of flat plate

E_p - effective modulus of elasticity of particulate

p - external pressure

r - radius of container r = 312 mm

t - thickness of titanium shell t = 4.76 mm

υ - Poisson's ratio

LAYOUT OF REPORT

The comprehensive report describing preparation, building and testing of the prototype, and evaluation of the test results is being issued in four parts:

Part 1 - Hydrostatic Tests - describes: tests conducted in preparation for building the prototype; prototype itself; inspection, assembly and instrumentation of the prototype; and hydrostatic test program.

Part 2 - Prototype Testing Following Hydrostatic Tests - describes: handling test; visual inspection following reopening of container; and metallographic evaluation.

Part 3 - Stress Analysis - describes: testing of titanium, particulate and other materials used in construction of the prototype; detailed stress analysis of "perfectly packed" container; analytical evaluation of the effects of voids.

Part 4 - Summary - a brief report outlining the work above and summarizing all results.

ontario hydro
research division

To H.N. Isaac
Manager
Nuclear Materials Management Dept.

TEST PROGRAM OF THE PROTOTYPE OF THE TWPP CONTAINER PART 1- HYDROSTATIC TESTS

1.0 INTRODUCTION

A thin-wall, particulate-packed (TWPP) container concept is being developed, as one of the Canadian alternatives for disposal of used fuel from the CANDU Nuclear Power Stations/1/. It is based on isolation of unreprocessed fuel bundles in an up to 1000 m deep repository in a thin-wall, particulate-packed titanium container as discussed in/2/. Under this concept, the used fuel bundles are placed in a thin, steel basket; the basket is then placed in a thin titanium shell, as shown in Fig. 1.

To improve the structural strength of the titanium shell, all void space inside the container will be filled with a particulate. The container is designed to:

(a) withstand a hydrostatic pressure of 10 MPa which might occur due to post-closure flooding of a 1000 m deep vault.

(b) resist corrosion (no penetrations in the shell) for up to 500 years,

(c) operate at temperatures up to 150°C.

The container is designed to contain up to 76 fuel bundles. This relatively complex design concept was selected in an effort to optimize the container cost and its strength, corrosion resistance and other external requirements.

The TWPP project is being conducted by Ontario Hydro as a part of the Ontario Hydro Technical Assistance Program (TAP) to AECL/3/. A prototype container was designed and acquired by the Mechanical Design Department/2/. The prototype was received by Research Division for extensive examination and testing. This report presents a chronological account of the prototype evaluation program together with tests' results, summaries and conclusions.

The comprehensive report describing preparation, building and testing of the prototype, and evaluation of the test results is being issued in four parts:

Part 1 - Hydrostatic Tests - describes: tests conducted in preparation for building the prototype; prototype itself; inspection, assembly and instrumentation of the prototype; and hydrostatic test program.

Part 2 - Prototype Testing Following Hydrostatic Tests - describes: handling test; visual inspection following reopening of container; and metallographic evaluation.

Part 3 - Stress Analysis - describes: testing of titanium, particulate and other materials used in construction of the prototype; detailed stress analysis of "perfectly packed" container; analytical evaluation of the effects of voids.

Part 4 - Summary - a brief report outlining the work above and summarizing all results.

This is Part 1 of the report.

The procurement of the prototype was preceded by extensive experimental and analytical programs, as discussed in References 4 through 6. These programs demonstrated that:

- all of the tested particulate materials flowed well and could fill all vacant spaces within and around bundles inside a TWPP container;
- none of the investigated particulates showed measurable creep under sustained pressure;
- all investigated particulates were found to have enough strength to structurally support the thin wall of the container under all postulated loads, see Appendix E;
- the stresses and strains in the container as analysed were not expected to approach the material's ultimate strength.

2.0 DESCRIPTION OF PROTOTYPE

The prototype container assembly is schematically illustrated in Figure 1. It consists of a thin titanium container and a steel basket. The container is made of several 4.76 mm thick plates rolled and welded together, as shown in Figure 2. All welds were brushed by manufacturer without our prior knowledge, making weld examination difficult. The mid-height, circumferential weld (in Figure 3) was polished as well. This weld was also locally undercut to a thickness of less than 4.76 mm. Because of this processing of welds, we were not able to determine by non-destructive examination what quality of welding was obtained. The welds will be evaluated in detail following the hydrostatic test program, and discussed in Part 2 of this report.

The top and bottom lids are shown in Figure 4. They were made by forming flat titanium plates 4.76 mm thick.

The prototype fuel basket consists of nineteen 4 in. schedule 10 pipes welded together, and welded to a spacer and to a spoke wheel used to support bundles. The Spacer ring used to position the basket in the container is illustrated in Figure 5. Figure 6 shows the spacer ring, spoke wheel and support ring. To provide the prototype container with a similar strength to that expected in an actual disposal container, 48 simulated fuel bundles were prepared. These largely simplified bundles provided an additional strength to the outer ring of the basket tubes. Strength of the outer row of tubes has the largest effect on container performance, as shown in the preliminary analyses/6/. They also provided larger resistance to particulate flow than the actual bundles would. A steel, simulated bundle is shown in Figure 7.

The particulate used in the assembly of the prototype was in the form of glass beads sieve size -18 to +25 or 0.71 mm to 1.00 mm diameter. Partial chemical composition of the glass is given in Table I.

Weight of the assembled prototype is shown in Table II.

3.0 ASSEMBLY OF CONTAINER

3.1 Shaker Table

A special shaker table was constructed, as shown in Figures 8 and 10. The table consists of two 36 in I-beams which provide the elevation so that actuator is attached near the containers' centres of gravity. The I-beams are reinforced by cross beams.

The beams on 30° angle, shown in Figure 8 are intended for the horizontal reinforcement of the actuator column. The dynamic part of the table consisted of a "shipping frame" enclosure in shape of a square structure of beams.

Linear bearings were used to ensure low friction between the static and dynamic parts of the table. The bearings are shown in Figure 11.

The actuator system (in Figure 12) used during compaction was part of the laboratory equipment normally used for seismic and fatigue tests. Compaction was achieved using sine wave excitation at accelerations of up to 4 g peak to peak in a horizontal direction only. Excitation in the vertical direction was not utilized because of the possibility of particulate flowing under the internal basket and floating it upwards, when accelerations of above 1 g were used. Figure 9 shows the test control panel used for input signal generation and test monitoring.

Both the Bristol and Ontario Hydro containers were successfully compacted/7/. A few minor difficulties encountered during the tests were overcome without significant delays or additional costs. The nature of those difficulties is presented below.

3.2 Particulate-Packed Container

The container was assembled. Forty-eight artificial bundles (see Figure 7) were inserted into the outer ring of the basket, as shown in Figure 13. Initially 635 kg (1400 lb) of particulate were used to fill the container. An additional 68 kg (150 lb) of particulate was added during vibratory compaction to retain the level of particulate 3/4 to 1 in above the basket.

In this test, a brief evaluation of packing was conducted at various frequencies and accelerations. The most significant packing was obtained at the frequency of 40 Hz and high acceleration.

The vibratory compaction consisted of the following stages:

- 7 min at 1.0 g peak-to-peak acceleration and 40 Hz frequency.

  Following this stage, basket was exposed, see Figure 14. An additional 22.7 kg (50 lb) of particulate was poured into the container.

- 3 runs of 2 min each at 2 g peak-to-peak acceleration and frequencies ranging from 10 to 100 Hz.

  After second 2-min run, the basket was again exposed (Figure 15) and more particulate was added (45 kg).

- 2 runs of 30 s each at 4 g peak to peak acceleration and frequency of 40 Hz.

  After these runs, the lid was inserted with particulate about 2.7 cm above the basket, as seen in Figure 16.

- 1.5 min at 4 g peak-to-peak acceleration and frequency of 40 Hz.

  The settlement achieved during the final 4 g test was about 0.5 cm (0.20 in). The effect of this settlement is shown by the pencil line in Figure 17.

The summary of the particulate packing process is presented in Table III.

The container was strain-gauged during the packing process. The largest strain measured during the vibratory compaction was 110×10^{-6}, resulting in a residual stress of 11 MPa (1,600 psi). During insertion of the top lid, an additional strain of 640×10^{-6} was introduced at the top of the vessel, producing an additional tensile stress of 64 MPa (9,300 psi).

3.3 Closure

The lid for the container was designed to fit with a relative ease. However, due to out-of-roundness shown in Figure 18, the lid required extensive hammering, to be put in place as seen in Figure 19. The final vibratory compaction was run with the lid in. After compaction, hammering was again used to determine the amount of the final settlement and to eliminate the resulting gap.

Following compaction, the lid was held in position by the centre bolt in the tripod, shown in Figure 20. The tripod was used to hold the lid firmly in place during handling and shipping. Ontario Hydro container's lid was welded at the Whiteshell Nuclear Research Establishment (WNRE).

The closure weld of the Ontario Hydro container showed significant air contamination in spite of the protective closure (see Figure 21). The unevenness of the weld and its discolouration can be seen in Figure 22.

4.0 SHIPMENT OF CONTAINER TO WNRE

The container with the shipping frame were too heavy for the crane available in the laboratory. The container was jacked up from the bearings.

Steel plates and air cushion pads provided by Aero-Go Inc were inserted under the container. Air pressure of 7 psi in the pads was adequate to move the container around. Difficulties were encountered because of air leaks on an uneven concrete floor or in the gaps between steel plates. Once a continuous line of plates with all gaps covered with masking tape was formed, the container was moved smoothly, as shown in Figure 23. Air cushion pads were used to remove the container out of the lab. A mobile crane placed it on the truck (Figure 24) for shipment to WNRE.

5.0 INSTRUMENTATION OF CONTAINER

The Ontario Hydro prototype container was extensively instrumented with both bondable and weldable (Ailtech type) strain gauges, to monitor deformation of the container during hydrostatic testing. Three thermocouples were installed to monitor temperatures at different elevations. The temperature was uniform throughout the vessel, during all tests and it was maintained at the required levels.

A special strain-gauge installation program for encapsulation of bondable gauges was undertaken by both Ontario Hydro and WNRE, because of the extreme environment seen by the container during the tests. During the tests, the containers were fully submerged in water at 150°C (300°F) and pressure of 10 MPa (1,450 psi). Both methods used multiple encapsulations including spot-welded metallic caps. The Ontario Hydro encapsulation method is shown in Figure 25, and discussed in detail in Reference 8.

The bondable gauges performed well during the preliminary tests at 10 MPa pressure and at temperatures of 100°C and 125°C. All six bondable gauges installed by WNRE performed well. Ontario Hydro method was used for installing 48 gauges. Only four of those gauges failed during the two preliminary tests. A large amount of data was obtained during those tests. The locations of all gauges used in these tests are shown in Figure 26.

During the 10 MPa, 150°C test, most of the bondable gauges failed. Only data from the Ailtech gauges has been collected, shown in Figure 27. The gauges failed mainly due to the high temperature. However, the preceding two thermal cycles could have damaged the gauges, contributing to their failure.

Additional weldable Ailtech type strain gauges were installed for the two tests with induced voids. The locations of all monitored gauges during these two tests are shown in Figures 29 and 30.

6.0 HYDROSTATIC TEST PROGRAM

Only one prototype is planned at this stage of the project. Thus, an extensive set of tests was designed to obtain as much information as possible from the prototype. The hydrostatic test program formed the main part of the prototype tests and it consisted of six stages as follows:

Stage 1. initial test at a temperature of 100°C and pressure of up to 10 MPa
Stage 2. second test at 125°C and 10 MPa
Stage 3. full temperature test at 150°C and 10 MPa
Stage 4. long term 16-day test at 150°C and 10 MPa
Stage 5. centre void test at 150°C and 10 MPa
Stage 6. side void test at 150°C and 10 MPa.

The results of the tests are usually presented in a graphical form showing strain (or displacement) as a function of pressure. These graphs are discussed in the following subsections and are included in Appendix C. The plots were generated by joining two consecutive measurements with a straight line. Curve fitting or curve smoothing techniques were not used.

6.1 Test Facilities

Whiteshell Nuclear Research Establishment (WNRE) has constructed a large pressure vessel, shown in Figure 31. After the prototype container was placed inside the vessel, the vessel was filled with chemically treated water. Only a small space was retained at the top of the upper head for pressurization. The vessel was pressurized using a six bottle bank of nitrogen bottles, shown in Figure 32. Test monitoring instrumentation consisted of Vishay 4000 data logging equipment controlled by HP 9825 microcomputer, seen in Figure 33. An HP85 microcomputer was also connected to the system to calculate principal stresses, as strain results became available. Other instrumentation used to monitor the container behaviour included three thermocouples connected to a digital thermometer and a manual strain indicator used for cross-checking the strain gauge readings.

6.2 Preliminary Tests

Instability of the cylindrical shell was anticipated at low pressures (below 0.25 MPa), as shown in Appendix F. The effect of buckling was minimized by the support provided by the parti-

culate. Several low pressure, ambient temperature of about 20°C cycles were conducted to determine if significant buckling occurred. The top lid was the only area where noticeable plastic deformations (up to 0.5 mm/m strain) occurred during the first low pressure cycle. All other strains measured during these cycles were very small, as shown in Table IV.

The lack of large deformations during these initial tests showed that the container did not have significant voids.

6.3 First-Stage Test

The first-stage test was conducted with the container heated to 100°C. An initial pressure of 0.5 MPa was applied to seal the pressure vessel. Strain gauge readings were taken every 0.25 MPa until the prssure of 5 MPa was reached and every 0.5 MPa above 5 MPa. A maximum pressure of 10 MPa was reached. During depressurization, measurements were taken every 1 MPa above 5 MPa pressure and every 0.5 MPa below 5 MPa. The test was completed successfully. Good strain and temperature measurements were obtained.

Results from the two different types of gauges are presented below. The consistency in results obtained from the two gauge types is illustrated in Plot 1 of Appendix C.

During preliminary tests, plastic deformations of up to 0.05% were observed after the 1 MPa test. These deformations were the result of the initial settlement of particulate throughout the vessel. During the first test to 10 MPa, the plastic deformation continued, as illustrated in Plot 2. Here, a permanent strain of 0.05 mm/m, or 0.005 mm/m per 1 MPa of pressure (average) was recorded at the rim of the top lid.

Large deformations were observed in the top lid, although strains measured at the gauge positions remained low. The top lid settled down from about 22.5 mm above the basket to about 7 mm, as illustrated in Figure 34.

Strains and deformations in the cylindrical shell depend on the elevation (proximity of discontinuities such as top and bottom lids or circumferential weld). Four different elevations are studied. Strains measured during pressurization, just below the top lid are shown in Plot 3. The plot shows the wide variation of strains around circumference. The average hoop strain of -3.3 mm/m is about twice the axial strain, which averages -1.8 mm/m.

The circumferential variation in results have not been explained fully. It is generally attributed to geometrical discontinuities (out-of-roundness, local flatness, thickness variations, etc) and metallurgical discontinuities (such as weld, different rolling pressure).

The gauges located 750 mm below the top of the cylindrical shell are considered to be adequately far from discontinuities and the end effects are negligible. Plot 4 shows strains at that location. The hoop strains are compressive at about -2 mm/m. The hoop strain near the axial weld (solid line on plot) is higher (-2.3 mm/m), apparently due to the discontinuity. Axial strain is near zero. Only small, positive strain was measured due to Poisson's effects. The reason for the low axial strain is presented in Appendix E, Section E-6.

A circumferential weld in the cylindrical shell is located about 1.5 m below the top. That weld has many inclusions and it was polished in several locations to a thickness lower than the parent metal (4.76 mm). The average hoop strain remains unchanged from the 750 mm location, as shown in Plot 5. Scatter of results is slightly larger, due to the discontinuities. A small, comressive axial strain was measured on the outside surface of the cylinder, near this discontinuity.

Strains near the bottom plate are shown in Plot 6. Total strains measured were less than 0.2% compression in the hoop direction and 0.03% tension in the axial direction. The axial tension is produced by Poisson's effects. The hoop strain is near the yield point.

6.4 Second Stage Test

For the second-stage test, the container was heated to 125°C, following sealing of the vessel at 0.5 MPa. Readings were taken during pressurization in the steps of 0.5 MPa. Last reading was taken at 9.5 MPa. When pressure reached 9.8 MPa, the seal on the pressure vessel failed and rapid depressurization occurred, as described in Appendix D. As a result of this accident, strain and temperature readings during depressurization are not available. The strains measured during the pressurization were generally lower than strains obtained during the first stage. Plots 7a and b show comparison of strains on the cylindrical shell. Strains on the top lid are presented in Plot 8.

Strains in the top lid away from rim are low and do not change significantly between tests (Plot 8a). This is attributed to the nearly parallel settlement of the top plate, as shown in Figure 34.

6.5 Full Pressure and Temperature Test

The third stage test was successfully conducted at 150°C. Full pressure of 10 MPa was achieved. Good strain and temperature measurements were obtained during pressurization and depressurization.

Plastic deformations were not seen during this stage, as illustrated for two locations in Plot 9. Some localized instabilities have been observed on the top plate. This is illustrated in Plot 10. We were unable to determine the cause of the instability. It could have been caused by the geometrical discontinuity at the top lid to cylindrical shell junction and/or by imperfect packing inside the lid radius.

6.6 Long Term Test

The fourth pressure cycle was made to demonstrate the "long term" stability of the container. The pressure vessel was heated to 150°C and pressurized to 10 MPa. The pressure was maintained without significant fluctuations for 16 days. An examination of the container following the test did not reveal any significant deformations. In most locations monitored, the strains were purely elastic.

The variation of strains due to the external pressure and time are shown in Plots 12 through 15. In the cylindrical shell, the pressurization and depressurization curves are similar. The time dependent curves (b) are close to straight, horizontal lines. The curve for location away from discontinuities shows slight discrepency between the two lines at high pressure. This is due to a further elastic deformation which occurred in the first thirty minutes after full pressure was reached, as shown in Plot 12b. The instability at the rim of top lid, seen during the previous stage, seems to significantly affect the early parts of this test. The strain pattern stabilized after seventh day of the test, as shown in Plot 14. This pattern could also be caused by water leakage to the strain gauge terminals.

6.7 Center Void Test

The container was well packed with particulate during the assembly at Ontario Hydro Research Division. Plastic deformations of the container were small. Under these circumstances, the possibility of container damage was remote.

A small void was introduced near the center of the top lid to assess the effect of imperfect packing. A small hole was drilled. After 370 g (0.21L) of particulate was vacuumed out, the hole was welded up, as shown in Figure 35. The void was

highly localized. It was about 15 mm deep and 125 mm in diameter. During the 10 MPa, 150°C hydrostatic test, a localized dent formed in the top lid. The diameter of the dent was about 250 mm. Depth at the void was up to 6 mm. The deformation around the void is shown in Figure 36.

Several additional strain gauges were installed near the void to monitor strains in the area, as shown in Figure 29. The strains at the void were significantly larger during this test than during previous 150°C tests, as shown in Plot 16. As we move away from the void, the strain difference disappears (see Plot 17).

This test has also demonstrated the integrity of the container. During drilling of the hole, it was found that the pressure inside the container was below atmospheric pressure. This partial vacuum was apparently the result of heating of the vessel during the closure welding. A similar vacuum was observed to a much lesser degree during subsequent drillings, as a result of plug welding. We believe that the maintenance of this partial vacuum during repeated pressure testing is strong evidence that the container remained sealed through all tests. Good sealing was further demonstrated by the dry particulate inside the container.

6.8 Side Void Test

The second void was also made in the top lid. The void was located near the cylindrical shell, see Figure 37. Significantly larger volume of glass beads was removed for this test: 1.64 kg (0.80 L). The void was again highly localized at the rim of the top lid. The hydrostatic test was run at 10 MPa and 150°C. The test produced large but localized deformations. Figure 38 shows two buckling waves in the cylindrical shell. The dent in the top lid is shown in Figure 39. The container retained its integrity and pressure boundry in spite of the deformations.

The large deformations produced large, non-linear strains near the void. As we move away from the void the strain patterns follow straight lines and are closer to the results of previous tests, when void was absent (see Plots 18 and 19).

7.0 COMPARISON OF TEST RESULTS WITH PRELIMINARY STRESS ANALYSIS

A preliminary stress analysis was conducted in the early stages of the design of the prototype/6/. The analysis was approximate because:

- the finite element models were simplistic and did not represent the geometry in an adequate detail;

- approximate values for properties of particulate were used;

- particulate was represented as a solid material, rather than a granular substance, as discussed in Appendix E;

- small displacements and linear-elastic material behaviour were assumed, even beyond the yield point.

Although the analysis was approximate, deformations of the same order of magnitude were obtained through tests and analysis, as shown in Table V. The analytically determined strains shown in the table combine local tensile or compressive and bending effects only. Effects of discontinuities such as welds, sharp corners, material imperfections are included in the experimental results, but not in the analytical results. The above mentioned simplifications and inaccuracies, in our opinion account for the large discrepencies in results.

Both methods indicate predominantly compressive strains throughout the titanium shell. The largest measured or calculated strains are within 4.1 mm/m. This is well within ultimate strain of 300 mm/m for titanium.

A more detailed analysis is planned for the near future and will form Part 3 of this report.

8.0 CONCLUSIONS

A protoype of the thin-wall, particulate-packed container has been successfully built, assembled and tested. The concept has been shown to be structurally viable. The tests have shown that:

- the container retains its structural integrity, even if large plastic deformations are present;

- the particulate has stiffness quite close to the stiffness of the cylindrical shell (see Appendix E);

- the particulate has an adequate strength to support the postulated pressures - no broken grains of particulate were observed;

- a good quality packing can easily be obtained. If small voids are present, they will not lead to violation of container integrity;

- although the quality of welding was below the standards specified for the container/9/, there were no problems that could be attributed to welding deficiencies.

Although structural adequacy of the container design has been shown, concept viability still depends on several other considerations, such as:

- adequacy of titanium to resist corrosion for the required period of time (500 years);
- corrosion should not be significantly accelerated by residual or pressure stresses equal to yield, at elevated temperature;
- acceptable welding and inspection procedures are established.

These issues are outside the scope of this report and are being addressed by other investigators.

9.0 ACKNOWLEDGEMENTS

The author wishes to thank Dr. J.D. Tulk for his assistance and valuable comments provided during preparation of this report. Messrs. A.Y. Cheung, M. Mikasinovic and R. Hoy of Design and Development Division designed and procured the prototype. Tests were conducted by Messrs. A.C. Fallis, J.H. Russell or OHRD and J. Barrie of WNRE. Nuclear Material Management Department provided funding and project coordination. The author acknowledges and thanks them for their input.

Recommended by:

J.A. Chadha
Area Co-Ordinator
Containment and
Immobilization Studies
Nuclear Waste Management
Program

Submitted:

B. Teper
Engineer
Applied Structural and Solid
Mechanics Section

Approved:

G.J. Clarke
Manager
Mechanical Research Dept

Reviewed By:

J.D. Tulk
Unit Head - Special Projects
and Computing
Applied Structural and Solid
Mechanics Section

BT:lg/sc/ds

REFERENCES

1. D.J. Cameron, "Fuel Isolation Research for the Canadian Nuclear Fuel Waste Management Program", Atomic Energy of Canada Ltd. Report, AECL-6834 (1982).

2. R. Hoy, M. Mikasinovic "Particulate-Packed, Thin-Wall Container - Prototype Design", Internal Ontario Hydro Report, June 9, 1981.

3. Joint Statement by Minister of Energy, Mines and Resources Canada and Ontario Energy Minister, June 5, 1978.

4. B. Teper, "Evaluation of the Design of Particulate-Packed, Thin-Wall Container for Disposal of Irradiated Fuel Bundles", CNS International Conference on Radioactive Waste Management, Winnipeg, Manitoba, Canada, September 12-15, 1982.

5. B. Teper, "Particulate Compaction Tests for a Particulate-Packed, Thin-Wall Container for Irradiated Fuel Disposal", AECL Report TR-131, December 1980.

6. B. Teper, "Preliminary Evaluation of Stress-Strain Distribution in Particulate-Packed Container", Ontario Hydro Research Division Technical Report 81-316-K, October 29, 1981.

7. M.H. Cooper and R. Tough, (L.J. Hosaluk, editor), "Phase II Design Report for a Structurally-Supported Used-Fuel Disposal Container", Atomic Energy of Canada Limited Technical Record, TR-222 (1984).

8. J. Russell, "Protection of Bondable Strain Gauges Under Severe Conditions (10 MPa Water 150°C) Using Sealed Cap Method", Ontario Hydro Research Division Report 83-481-K, December 23, 1983.

9. Tender Documentation for Purchase of the Thin-Wall, Particulate-Packed Container 0821 TW 70300 27, dated July 31, 1981.

APPENDIX A

TABLES

Table I	Chemical Composition of Glass
Table II	Weight of Prototype
Table III	Packing Test
Table IV	Strains During Low Pressure Tests
Table V	Comparison of Experimental and Analytical Results

TABLE I

CHEMICAL COMPOSITION OF GLASS

Composition	Fraction by Weight (%)
Silicon Oxide	37.8
Calcium Oxide	14.1
Sodium Oxide	0.9

TABLE II

WEIGHT OF PROTOTYPE

Component	Weight of Prototype		Weight of Disposal Container	
	N	lbs	N	lbs
Container Shell	1,110	250	890	200
Basket	4,360	980	4,360	980
Bundles	8,240	1,850	16,750	3,770
Glass Beads	6,670	1,500	5,550	1,250
Total Container	20,380	4,580	27,550	6,200
Shipping Frame	11,520	2,590		
Shipping Weight	39,900	7,170		

TABLE III
PACKING TEST

Step	Container Acceleration 1)	Frequency (Hz)	Duration (min)	Settlement (cm)	Level Above Basket (cm)		Comments
					Before	After	
1	0.5	40	7	2.5	2.5	0.5	22.7 kg of Beads Added
2	2.0	20	2	2.0	2.5	1.0	Centre Plate Showing (See Fig. 13)
3	2.0	40	2	3.0	1.0	-1.0	Basket Exposed (See Fig. 15)
4	2.0	70	2	1.0	4.5	4.0	45.4 kg of Beads Added Before Running
5	2.0	100	2	0.5	4.0	3.5	
6	4.0	40	0.5	0.5	3.5	3.0	
7	4.0	40	0.5	0.5	3.0	2.7	Lid Inserted
8	4.0	40	1.5	0.5	2.7	2.5	

Notes:

1. *Sinusoidal acceleration was applied, symmetrical about zero. Values given are peak to peak, expressed in g's.*
2. *The height of particulate above basket is about 2.0 cm at the time of shipment.*

166269 RD

TABLE IV
STRAINS DURING LOW PRESSURE TESTS

Cycle	Pressure (MPa)	Max. Pressure During Cycle	Strain in Typical Locations (x 10^6)									
			Top Lid				Cylindrical Shell					
			Centre		Rim		At Top Lid		Mid Height		At Bottom	
			Radial	Hoop	Radial	Hoop	Axial	Hoop	Axial	Hoop	Axial	Hoop
1	0.0	1.0	0.0	0.0	0.0	0.0	0.0	0.0	0.0	0.0	0.0	0.0
	0.4		544	-338	911	-450	-55	-282	4	-88	31	-94
	1.0		919	-230	817	-542	-160	-492	2	-221	50	-208
	0.0		395	-235	509	-204	0	-114	0	-28	17	-29
3	0.0	0.4	0.0	0.0	0.0	0.0	0.0	0.0	0.0	0.0	0.0	0.0
	0.4		538	-101	770	-417	-63.0	-281	6.0	-112	28.0	-107
	0.0		-101	-104	193	-90	0.0	-41	0.0	-8	0.0	-10
	0.0*		-26	-32	49	-33	0.0	-11	0.0	-1	0.0	-3

* 28 min. after end of test container returned to its original shape.

TABLE V

COMPARISON OF EXPERIMENTAL AND ANALYTICAL RESULTS

Shell	Location	Direction	Strain (mm/m)	
			Experimental	Analytical
Top Plate	Centre		0.23	-0.9
Top Plate	Rim	Hoop	-0.70	-1.4
Cylindrical	Top Rim	Hoop	-4.10	-3.3
		Axial	-2.20	-0.2
	Middle	Hoop	-1.80	-3.3
		Axial	0.10	-0.1
	Bottom	Hoop	-1.70	-1.8
		Axial	0.20	-1.9

APPENDIX B

FIGURES

Figure 1 Thin-Wall, Particulate-Packed Container

Figure 2 Prototype Container

Figure 3 Mid-Height Circumferential Weld

Figure 4 Top Plate

Figure 5 Basket

Figure 6 Basket Details

Figure 7 Simulated Bundles

Figure 8 Bristol Container Before Packing

Figure 9 Shaker Table Control Panels

Figure 10 Shaker Table

Figure 11 Linear Bearings

Figure 12 Actuator System

Figure 13 Basket with Artificial Bundles

Figure 14 Exposed Basket After Initial Packing (First Run)

Figure 15 Exposed Basket After Third Run

Figure 16 Level of Particulate Before Inserting Lid

Figure 17 Lid in Position - Final Settlement

Figure 18 Lid-Container Misalignment

Figure 19 Inserting the Lid

Figure 20 Top Lid Prepared for Shipping

Figure 21 Protective Chamber Used for Closure Weld

Figure 22 Closure Weld

Figure 23 Removal of OH Container

Figure 24 On the Way to WNRE

Figure 25 Sealed Cap Gauge Protection System

Figure 26 Location of Strain-Gauges During Preliminary Tests

Figure 27 Location of Monitored Gauges During the 150°C Test

Figure 28 Location of Gauges During the 16-day Test

Figure 29 Location of Gauges - Test of Center Void

Figure 30 Location of Gauges - Test of Side Void

Figure 31 Pressure Vessel for Hydrostatic Test

Figure 32 Test Facility

Figure 33 Test Monitoring Equipment

Figure 34 Permanent Deformation of Top Lid During First-Stage Test

Figure 35 Formation of Center Void

Figure 36 Deformation of Top Lid Following Test with Center Void

Figure 37 Location of Two Voids (Plugs)

Figure 38 Buckling of Cylindrical Shell due to Rim Void

Figure 39 Deformation of Top Plate at Rim Void

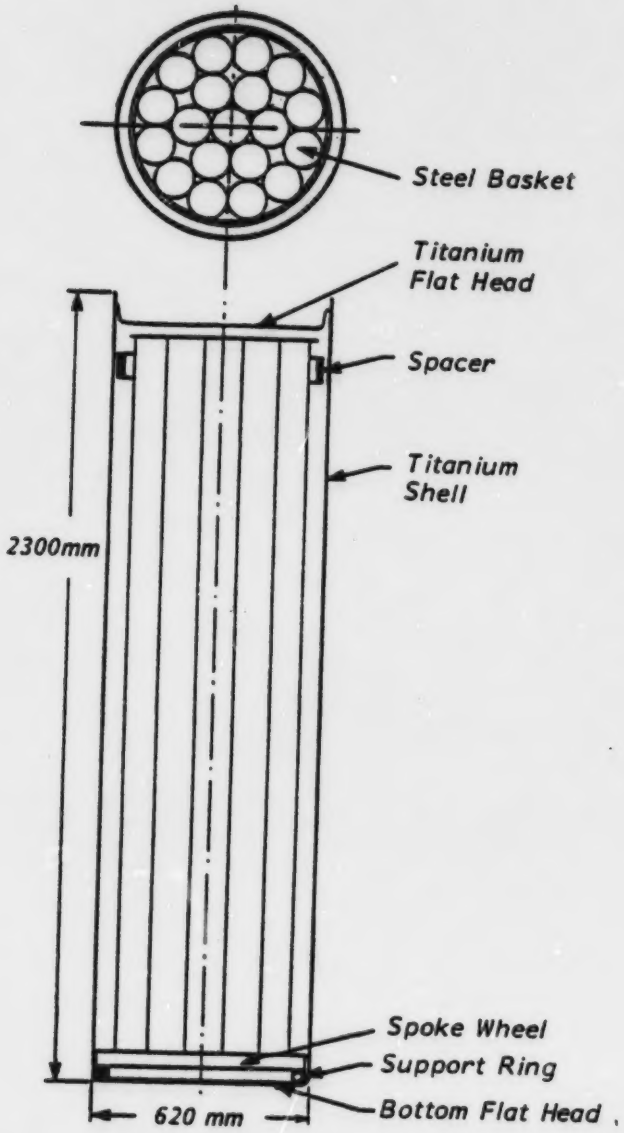

FIGURE 1
THIN-WALL PARTICULATE-PACKED CONTAINER

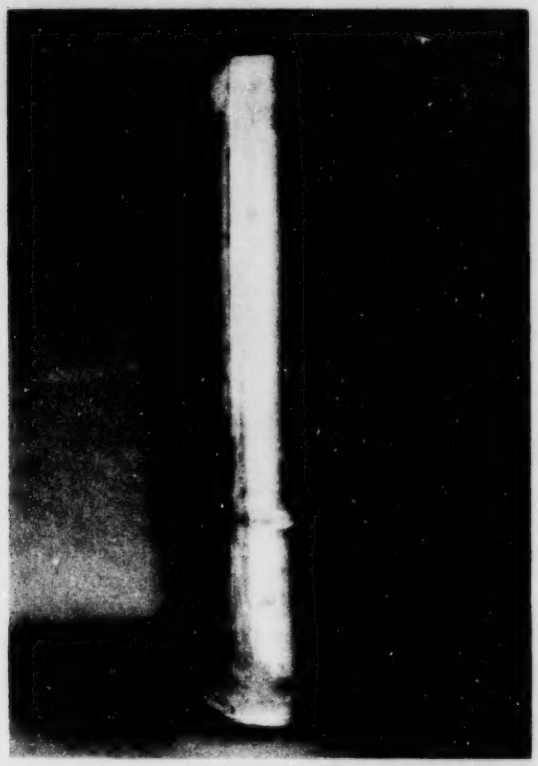

(a)

(b)

FIGURE 2
PROTOTYPE CONTAINER

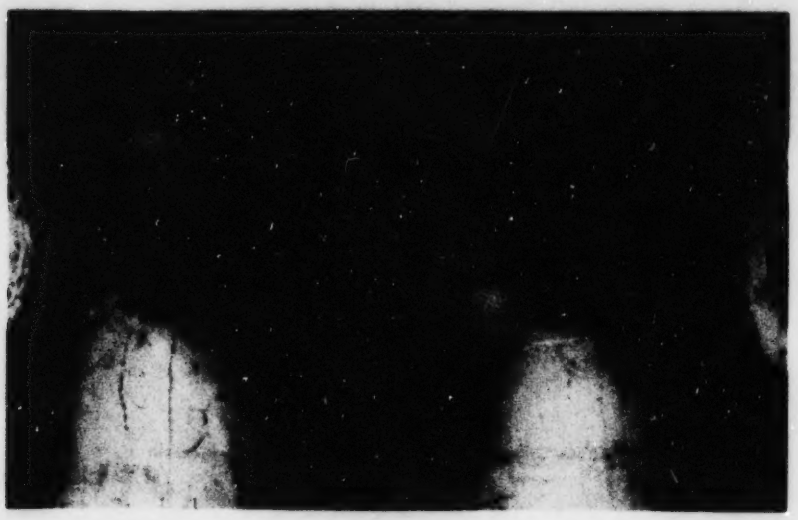

FIGURE 3
MID-HEIGHT, CIRCUMFERENTIAL WELD

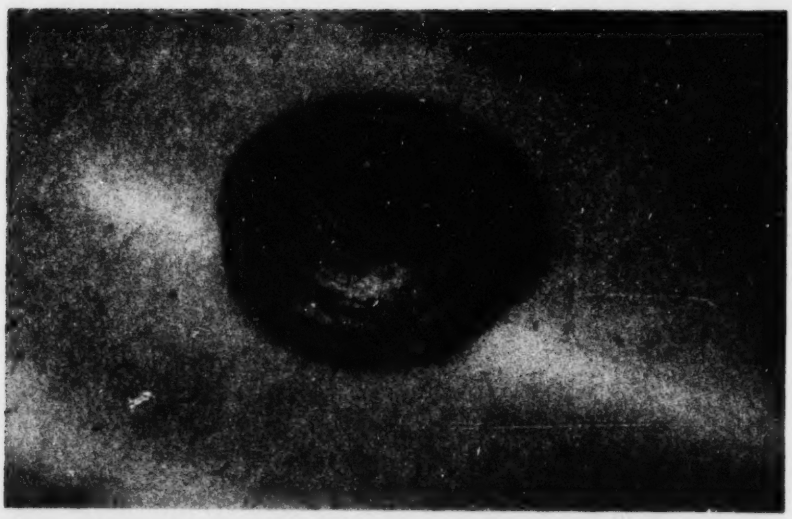

Note: Bottom plate is identical except slightly larger in diameter.

FIGURE 4
TOP PLATE

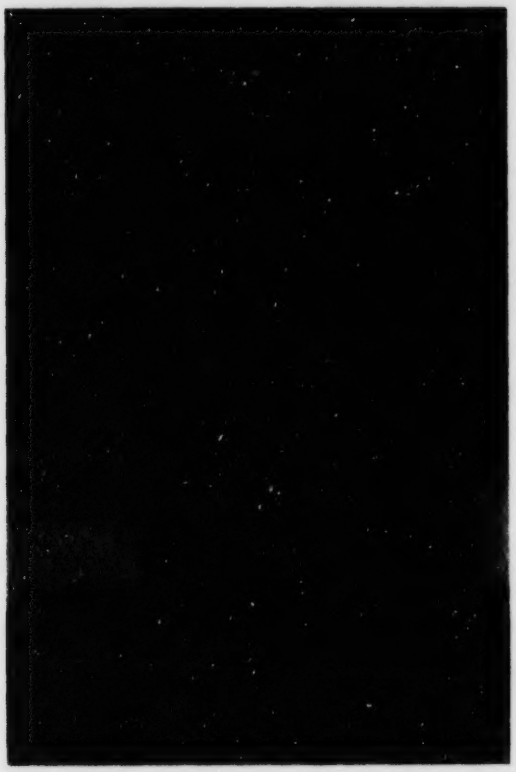

FIGURE 5
BASKET

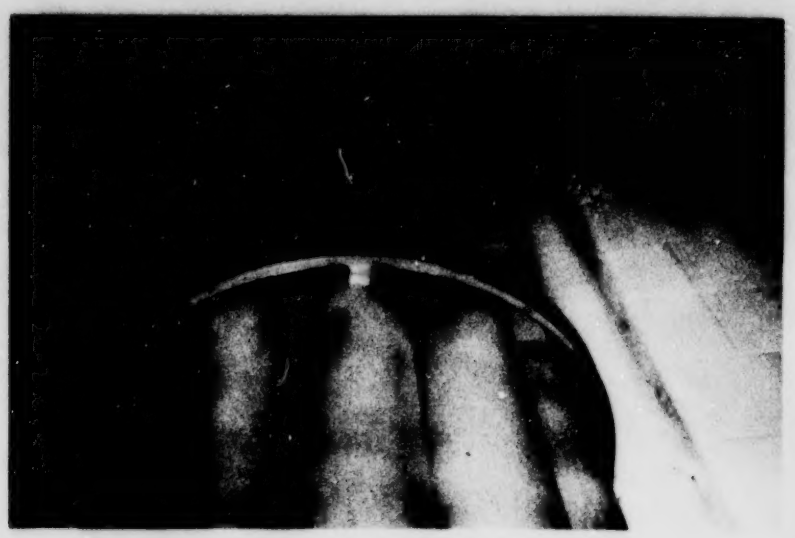

(a) Spacer Ring

(b) Supporting Ring and Spoke Wheel

FIGURE 6
BASKET DETAILS

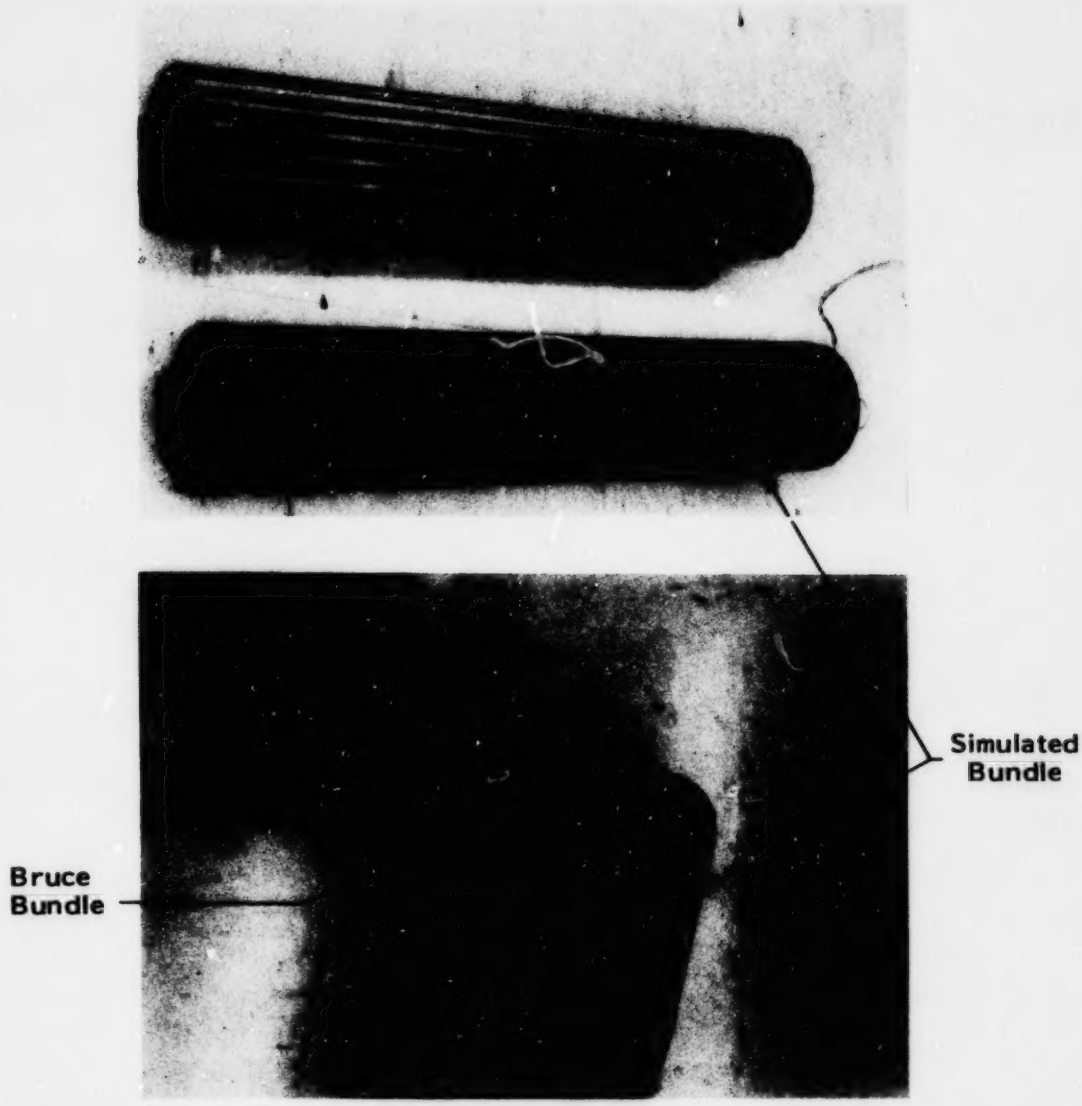

FIGURE 7
SIMULATED BUNDLES

FIGURE 8
SHAKER TABLE - PLAN VIEW

FIGURE 9
SHAKER TABLE CONTROL PANELS

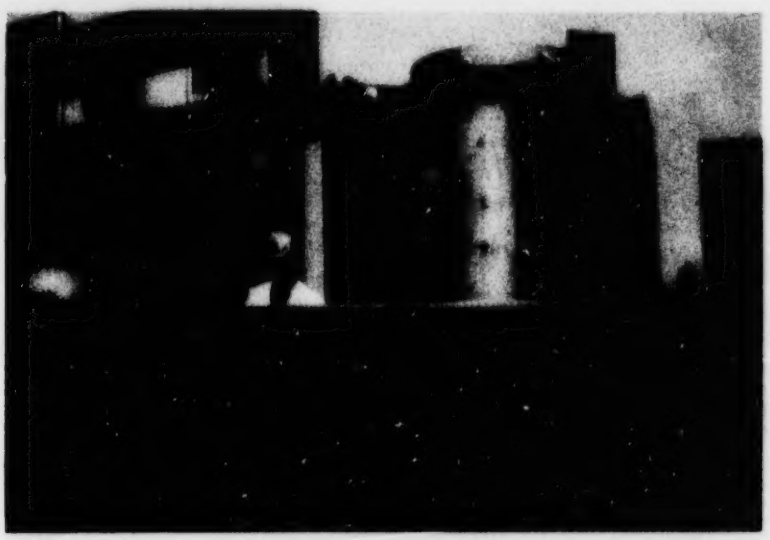

(a) Side View

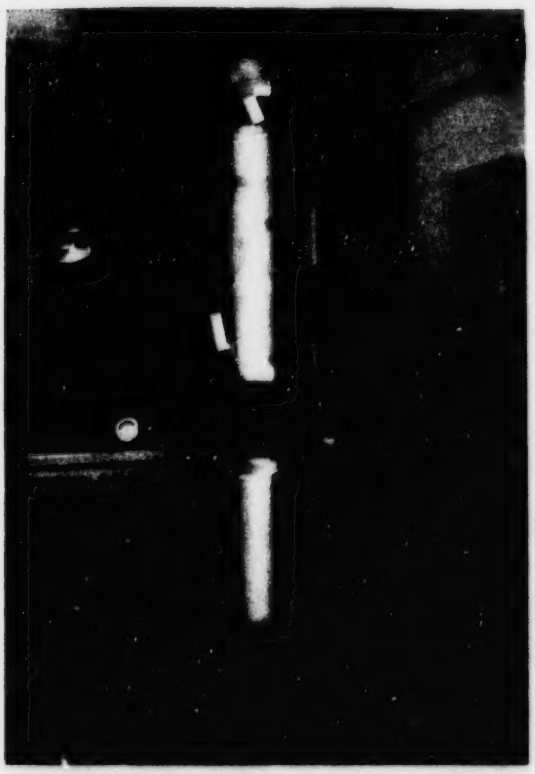

(b) Rear View

FIGURE 10
SHAKER TABLE

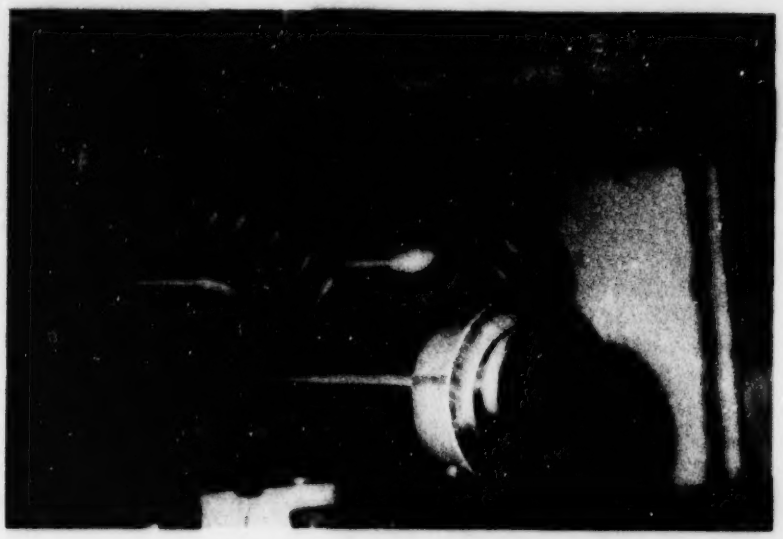

(a) Right-side Bearing

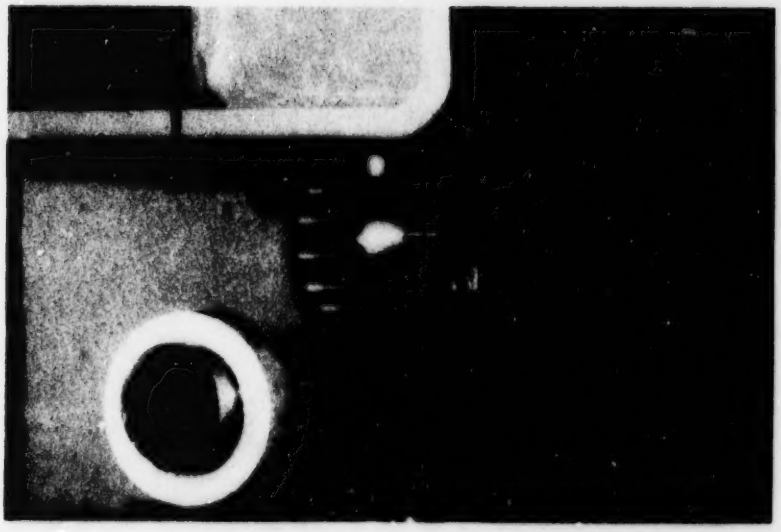

(b) Left-side Bearing

FIGURE 11
LINEAR BEARINGS

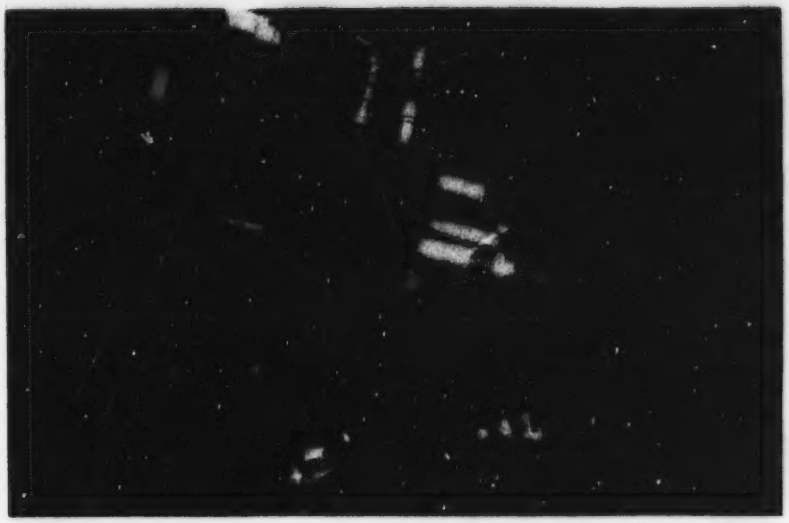

FIGURE 12
ACTUATOR SYSTEM

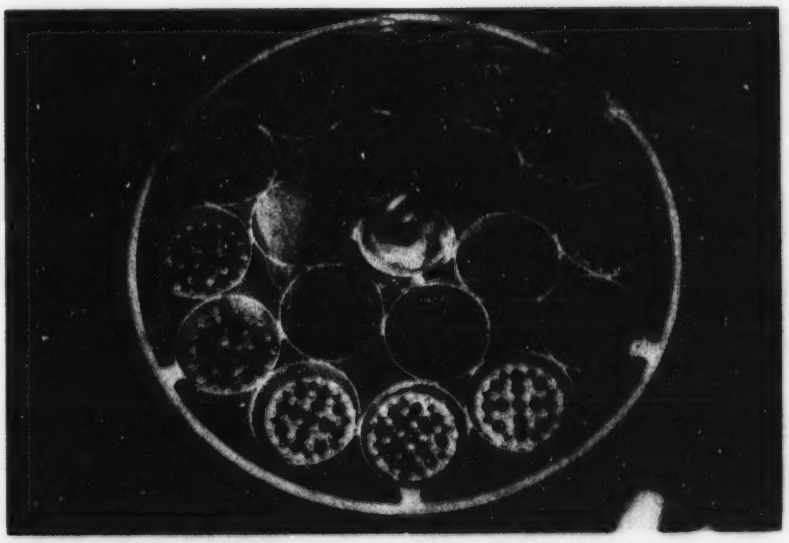

FIGURE 13
BASKET WITH ARTIFICIAL BUNDLES

FIGURE 14
EXPOSED BASKET AFTER INTIAL PACKING (FIRST RUN)

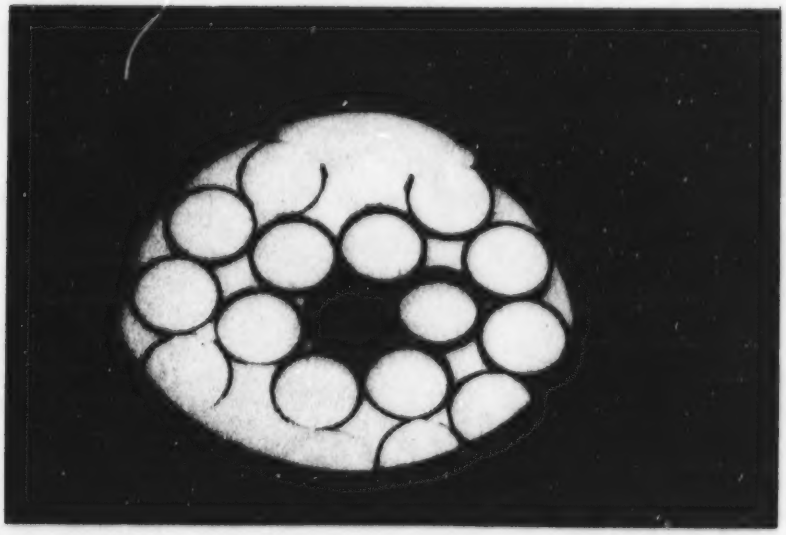

FIGURE 15
EXPOSED BASKET AFTER THIRD RUN

FIGURE 16
LEVEL OF PARTICULATE BEFORE INSERTING LID

FIGURE 17
LID IN POSITION - FINAL SETTLEMENT

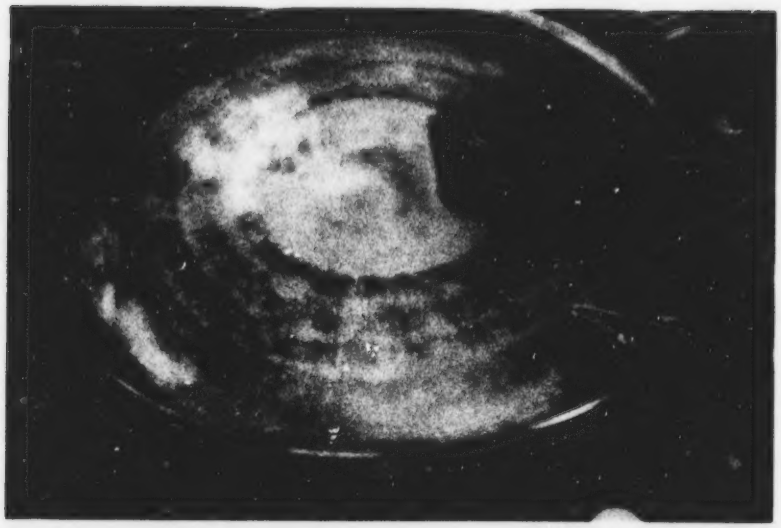

FIGURE 18
LID-CONTAINER MISSALIGNMENT

FIGURE 19
INSERTING THE LID

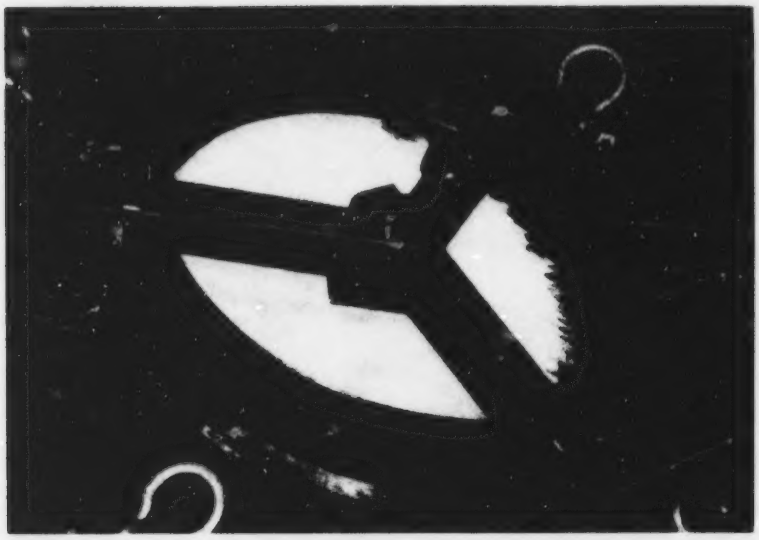

FIGURE 20
TOP LID PREPARED FOR SHIPPING

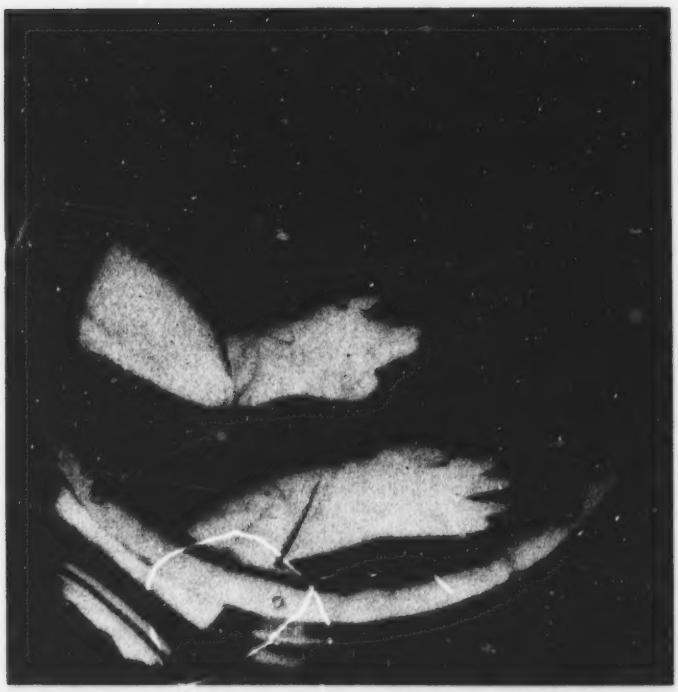

FIGURE 21
PROTECTIVE CHAMBER USED FOR CLOSURE WELD

FIGURE 22
CLOSURE WELD

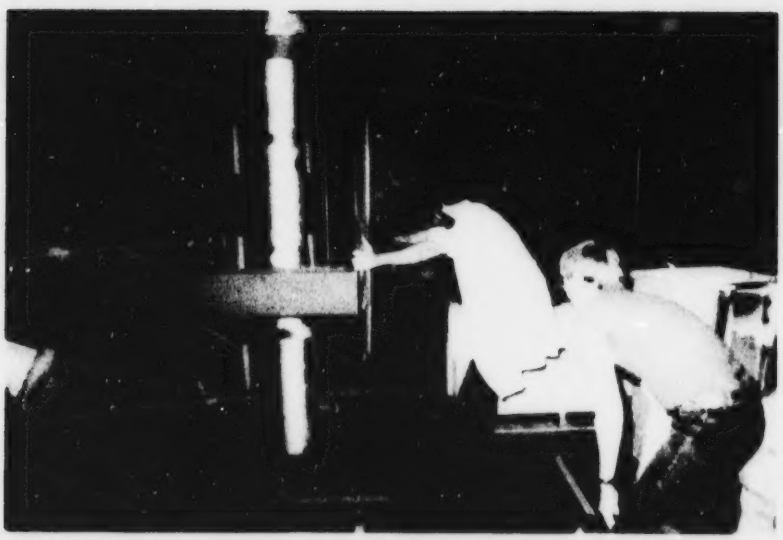

FIGURE 23
REMOVAL OF O.H. CONTAINER

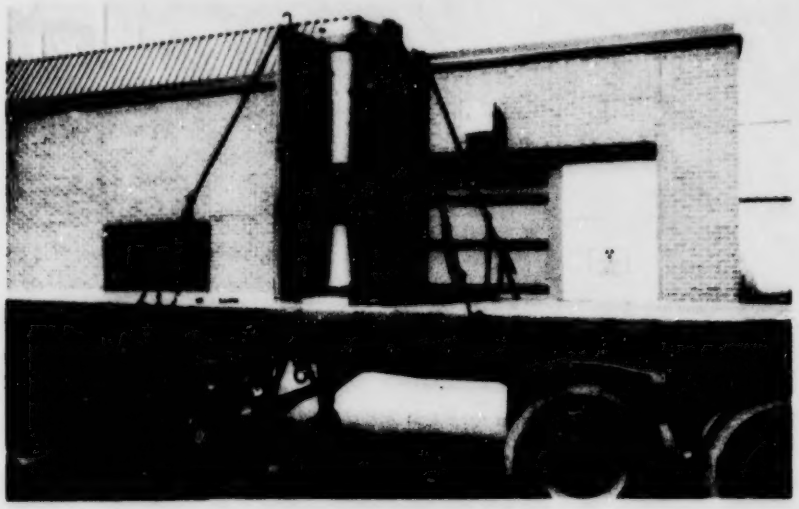

FIGURE 24
ON THE WAY TO WNRE

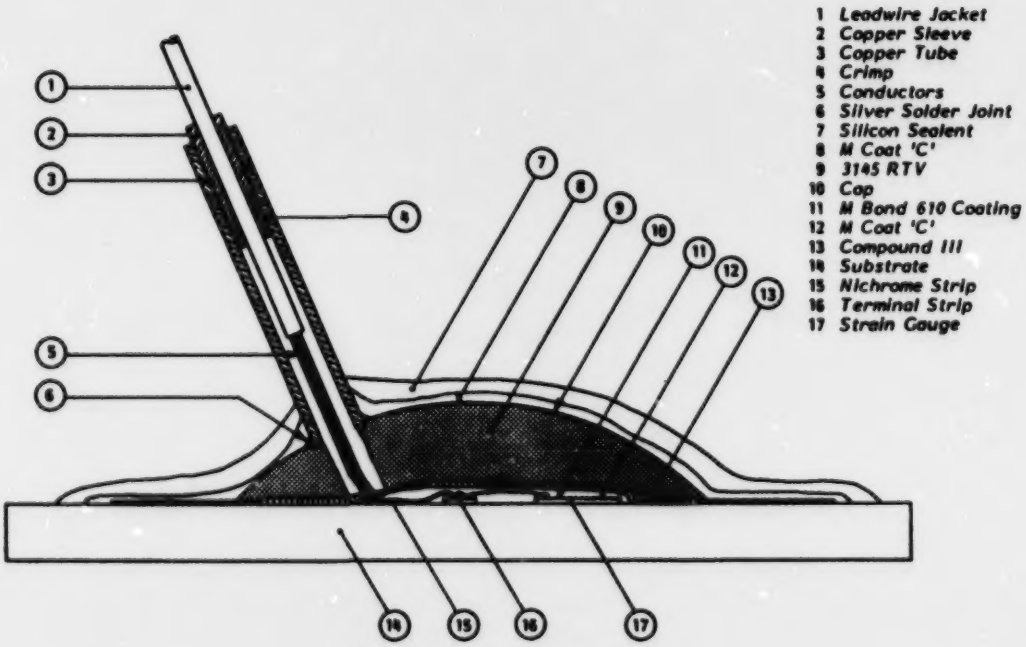

FIGURE 25
SEALED CAP GAUGE PROTECTION SYSTEM

Reprinted from Reference 8.

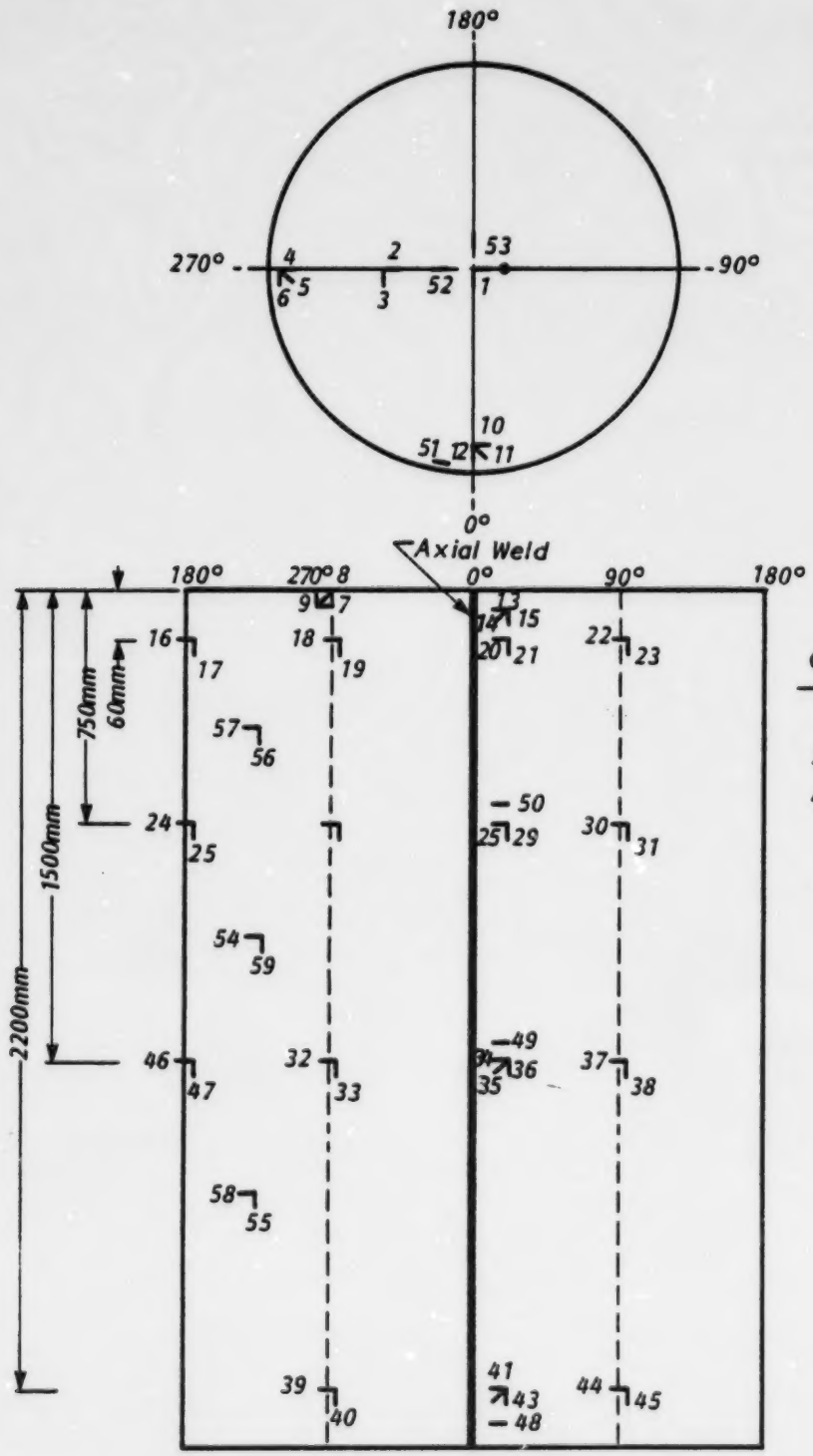

FIGURE 26

LOCATION OF STRAIN GAUGES
DURING PRELIMINARY TESTS

166288 RD

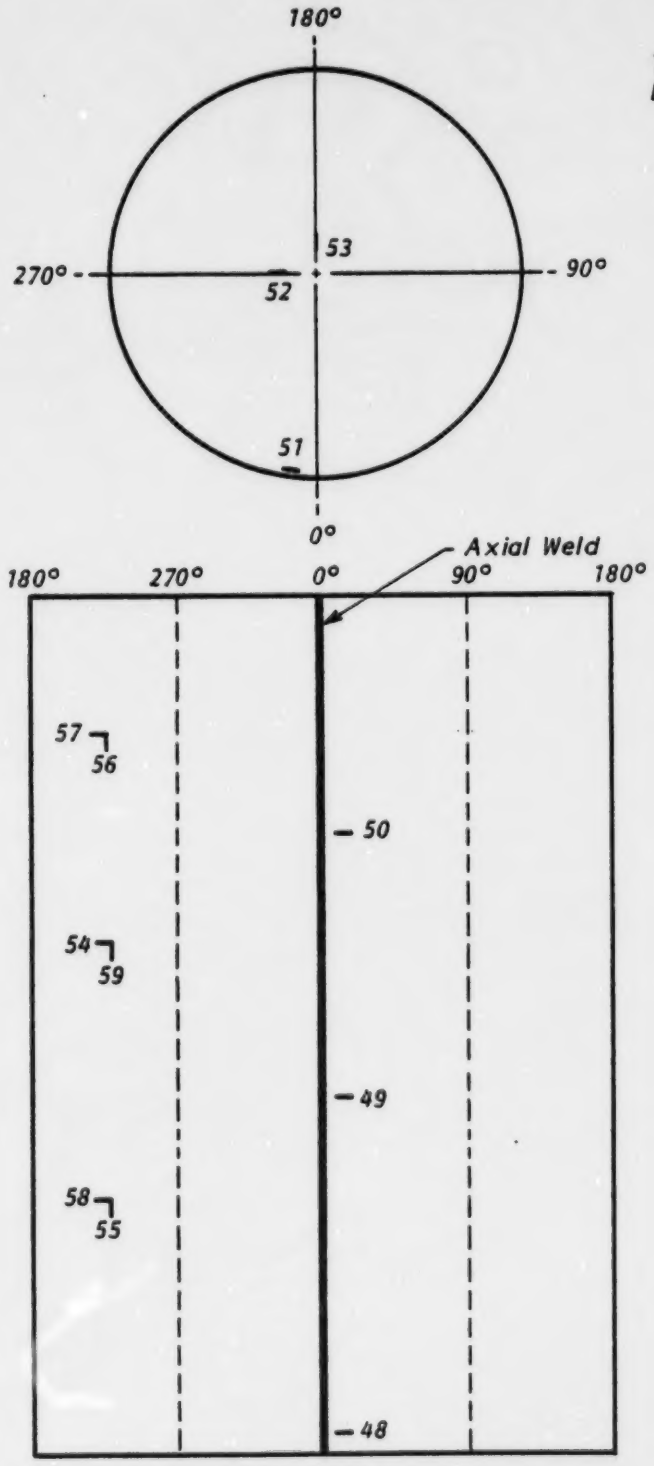

Test: 150°C (4 hrs)
Date: Oct 13, 1983

48 - 53 Ailtech Gauges
54 - 59 WNRE Gauges

FIGURE 27

LOCATION OF MONITORED GAUGES
DURING THE 150°C TEST

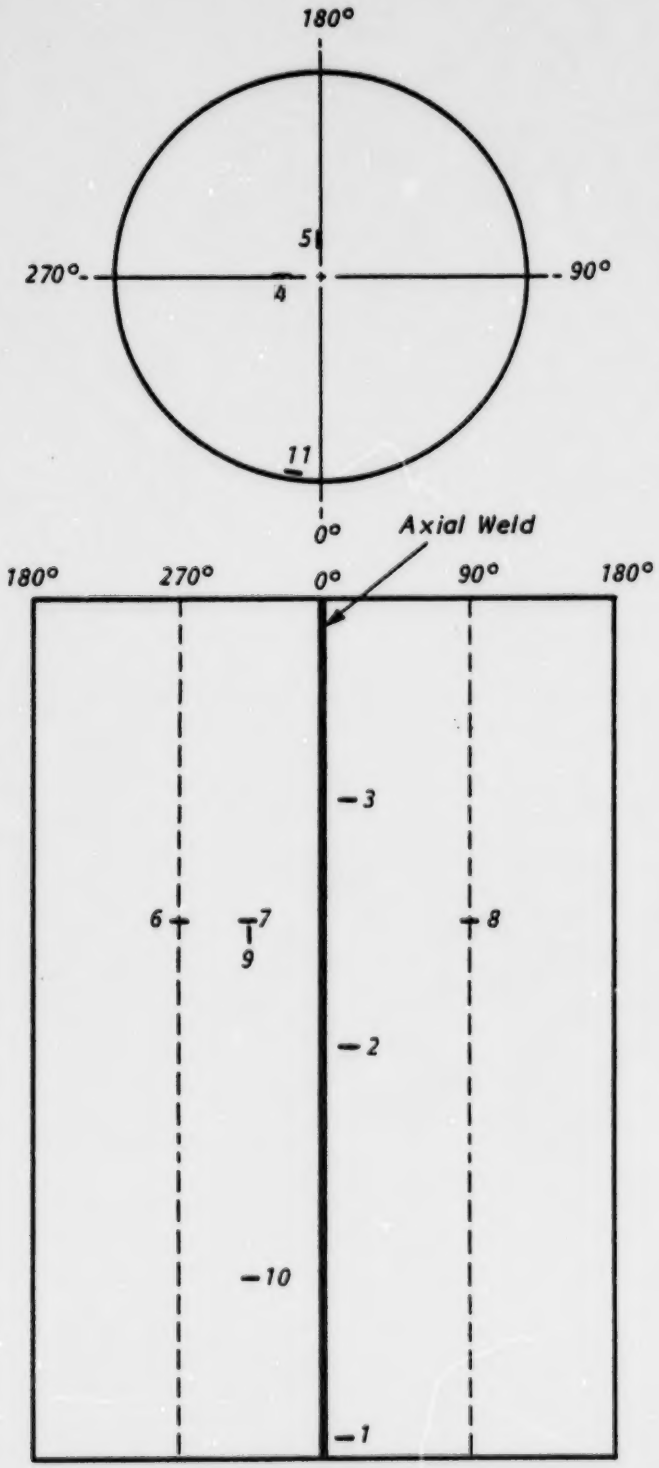

Test: 150°C (16 Day)
Date: Oct 31 - Nov. 15, 1983

1 - 11 Ailtech Gauges

FIGURE 28
LOCATION OF GAUGES
DURING THE 16 DAY TEST

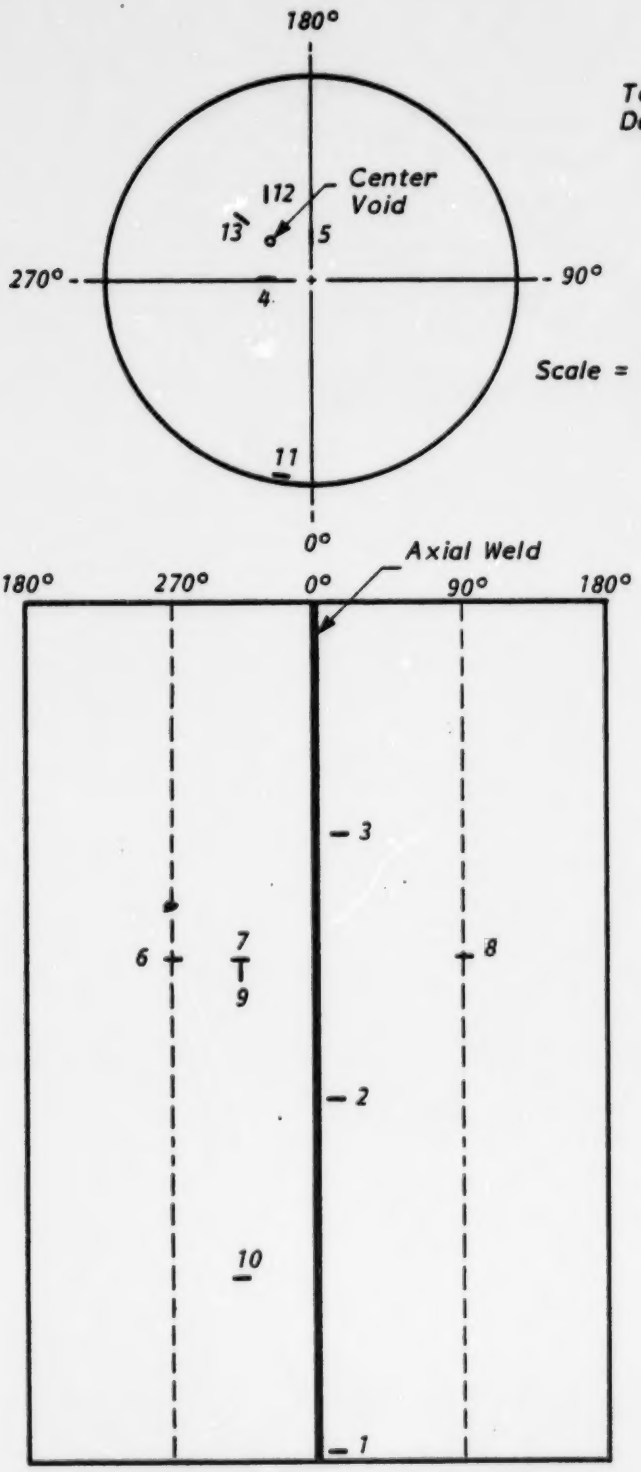

FIGURE 29

LOCATION OF STRAIN GAUGES -
TEST OF CENTER VOID

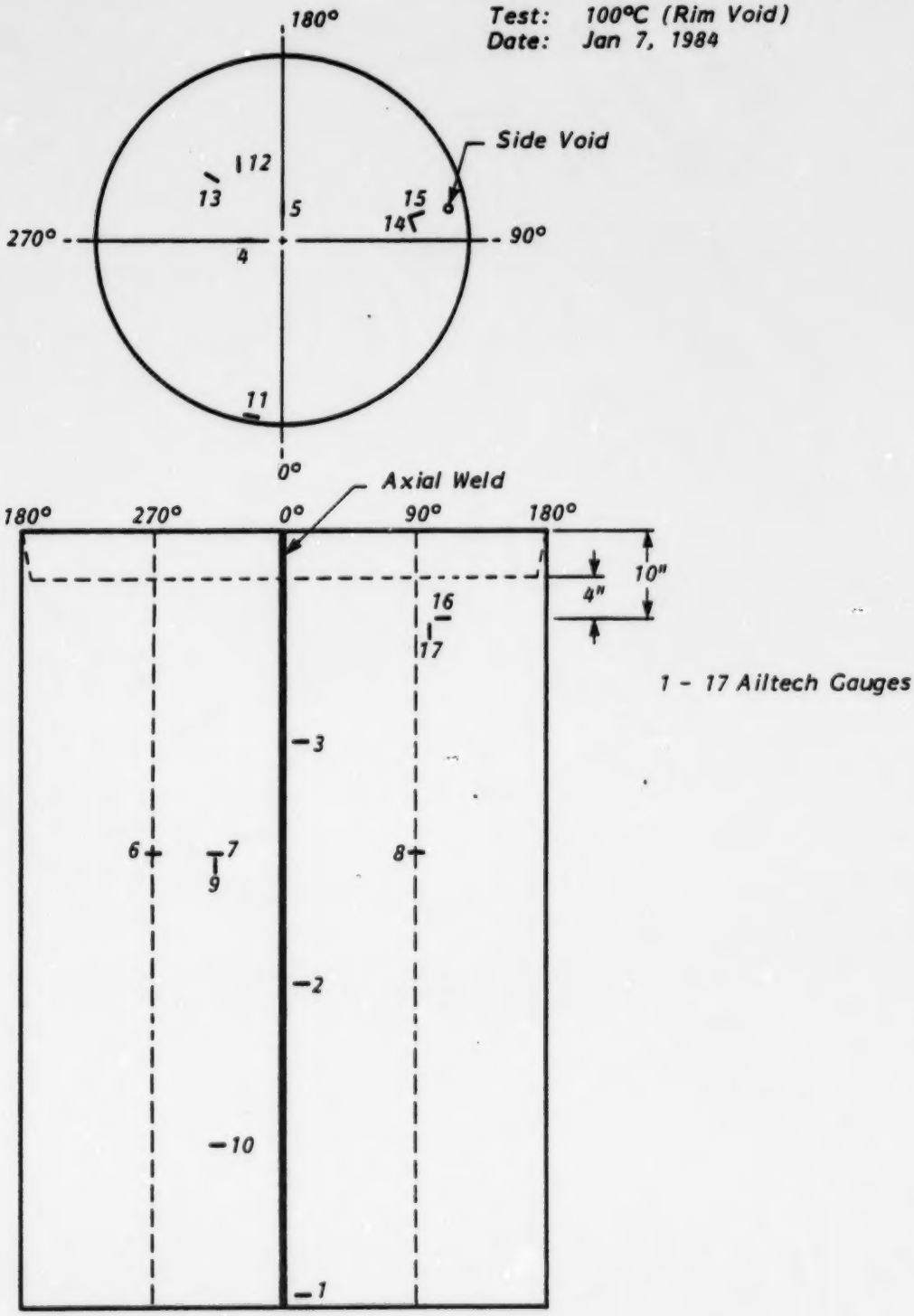

FIGURE 30

LOCATION OF STRAIN GAUGES
DURING TEST WITH SIDE VOID

166292 RD

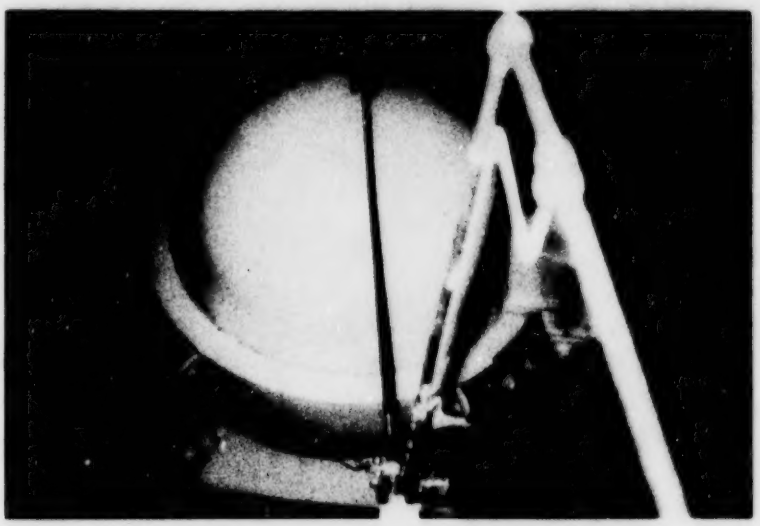

(a) Outside View

(b) Inside View

FIGURE 31
PRESSURE VESSEL FOR HYDROSTATIC TEST

FIGURE 32
TEST FACILITY

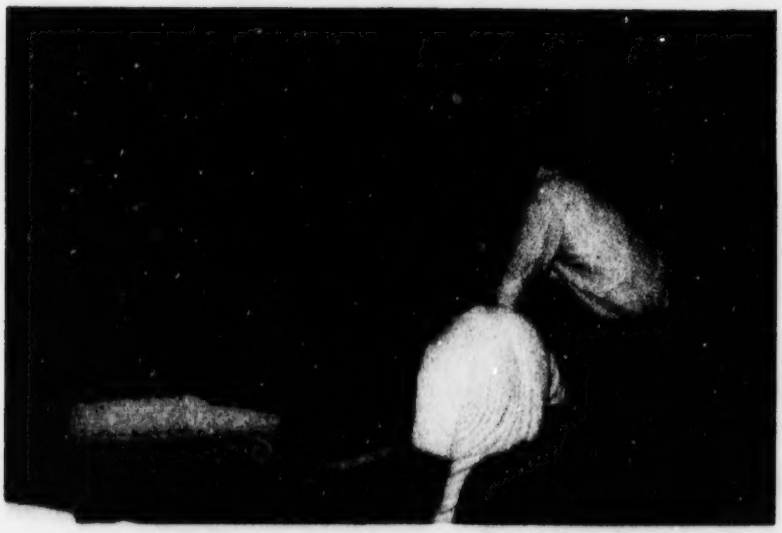

FIGURE 33
TEST MONITORING EQUIPMENT

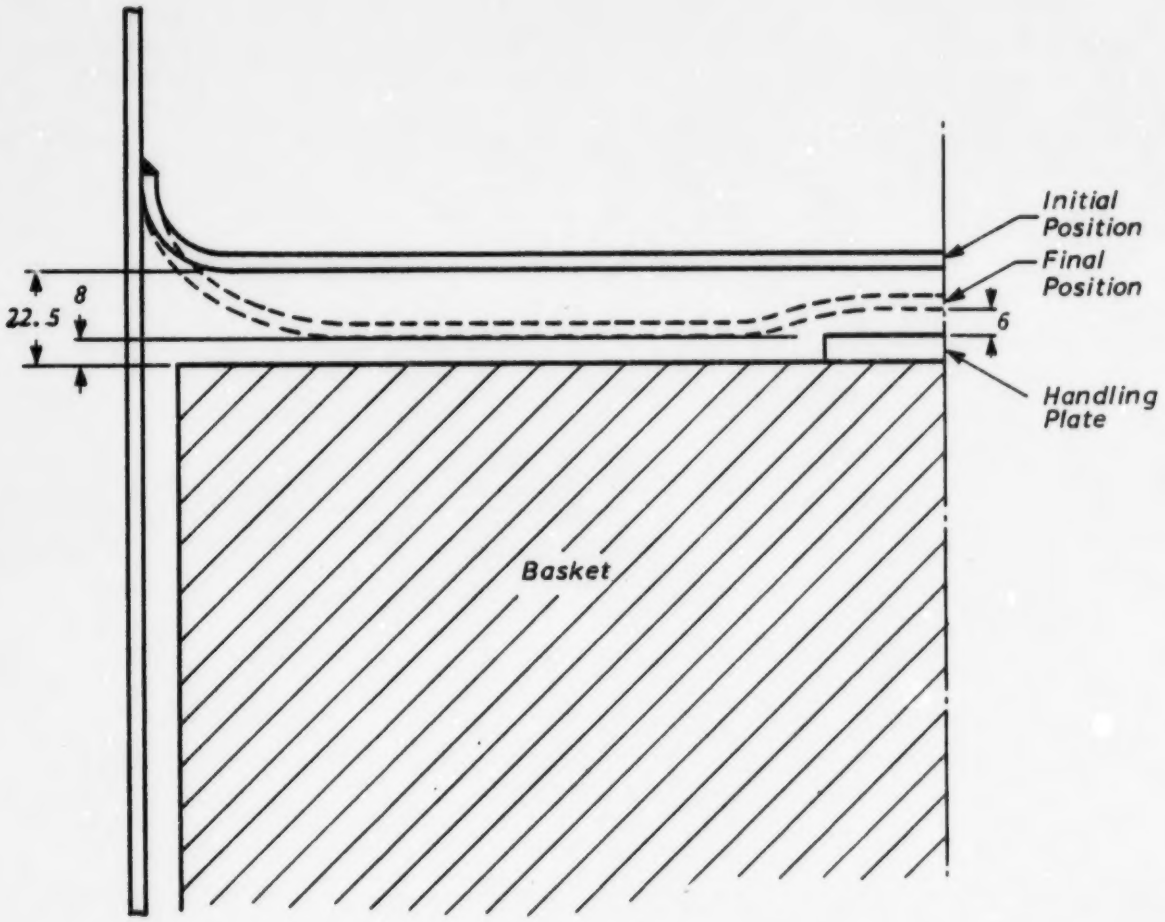

All Dimensions are in Millimeters

Not to Scale

FIGURE 34

PERMANENT DEFORMATION OF TOP LID
DURING FIRST-STAGE TEST

(a) Hole Drilled to Remove Particulate

(b) Location of The Centre Plug

FIGURE 35
FORMATION OF CENTRE VOID

(a) Deformation Pattern in Radial Direction

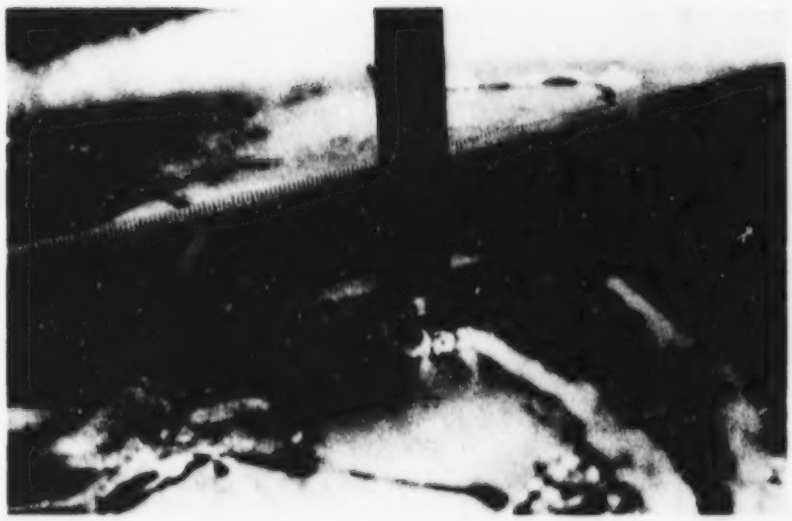

(b) Deformation Pattern in Circumferential Direction

FIGURE 36

DEFORMATION OF TOP LID FOLLOWING TEST WITH CENTRE VOID

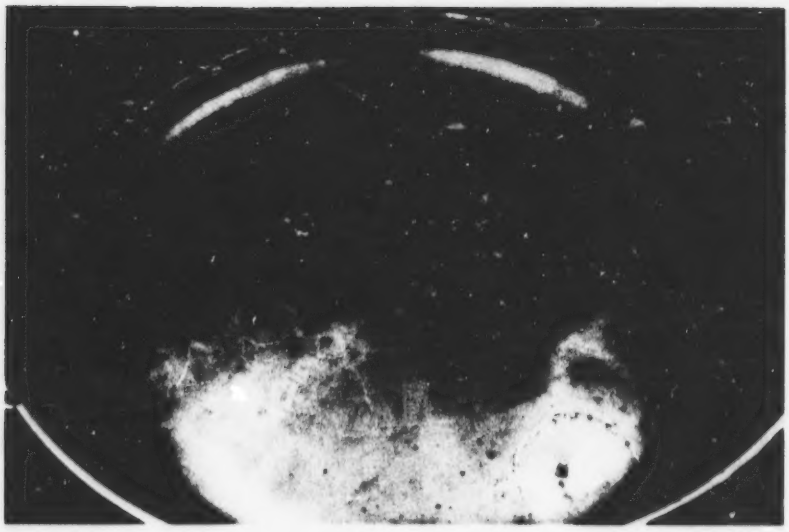

FIGURE 37
LOCATION OF TWO VOIDS (PLUGS)

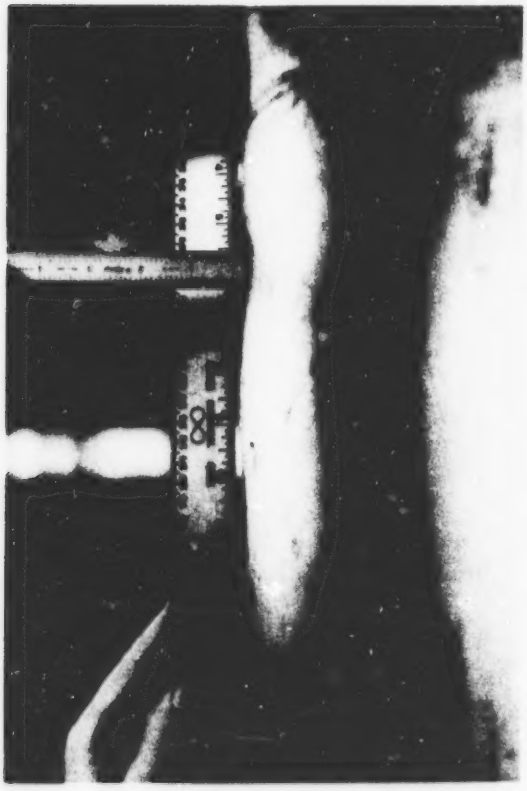

FIGURE 38
INSTABILITY OF CYLINDRICAL SHELL
DUE TO RIM VOID

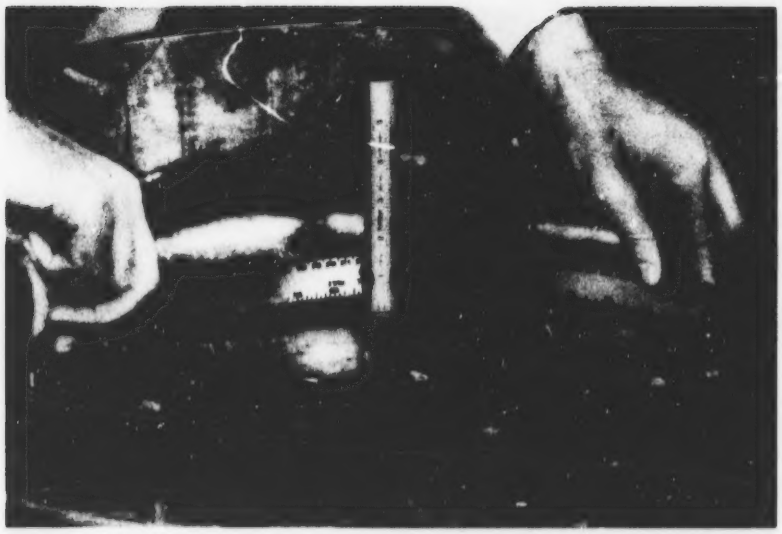

(a) Circumferential Direction

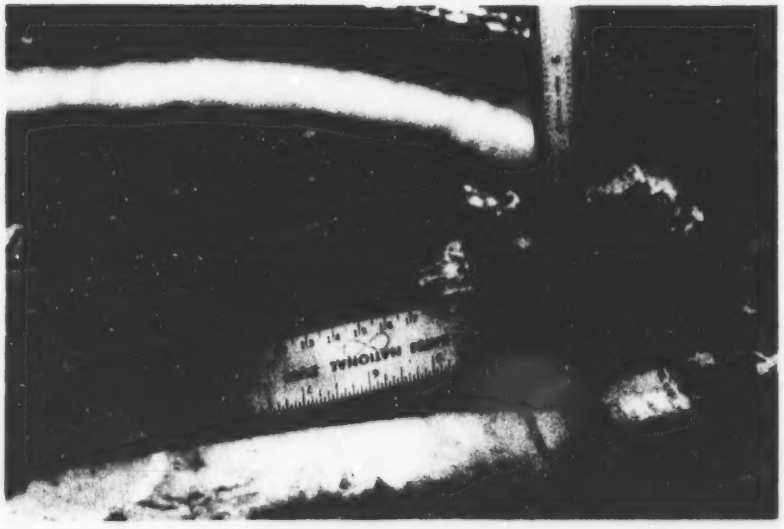

(b) Radial Direction

FIGURE 39
DEFORMATION OF TOP PLATE AT RIM VOID

APPENDIX C

HYDROSTATIC TEST RESULTS

(Plots)

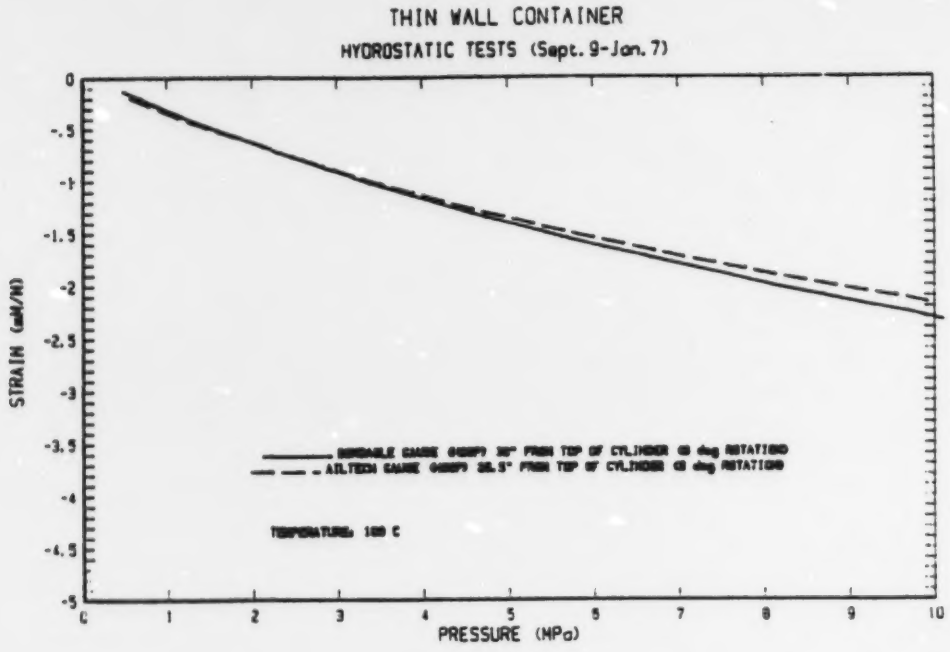

PLOT 1

RESULTS FROM BONDABLE AND WELDABLE GAUGES - SIMILAR LOCATIONS

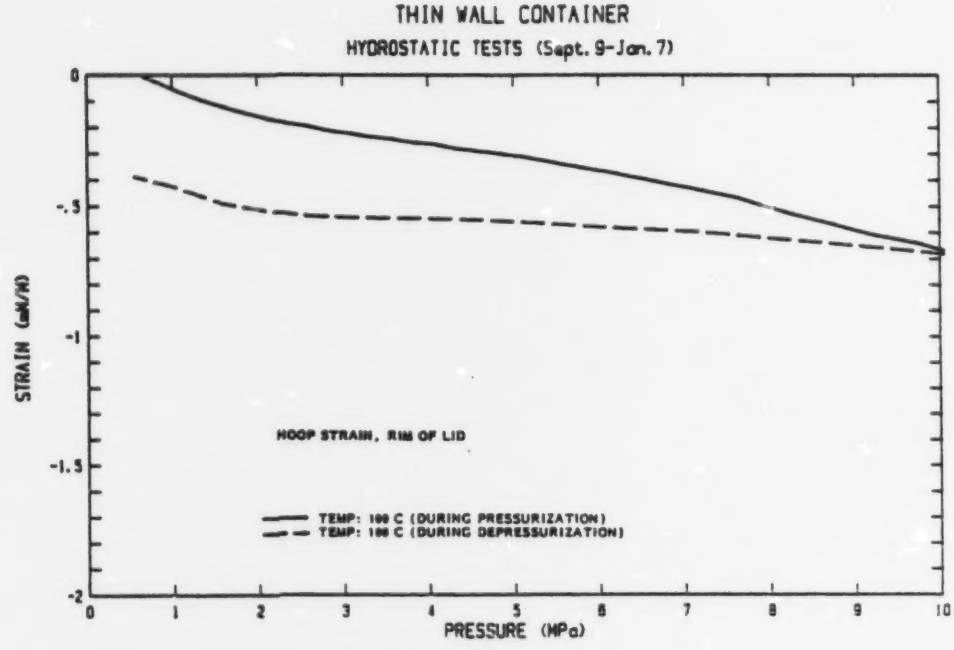

PLOT 2

PLASTIC DEFORMATION DURING FIRST-STAGE TEST

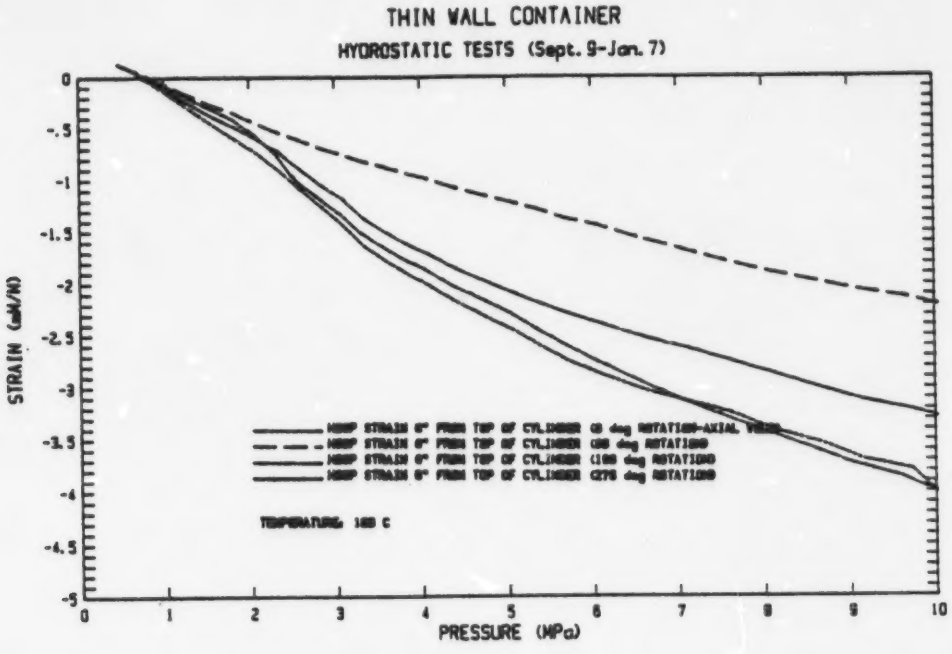

(a) Hoop Strain

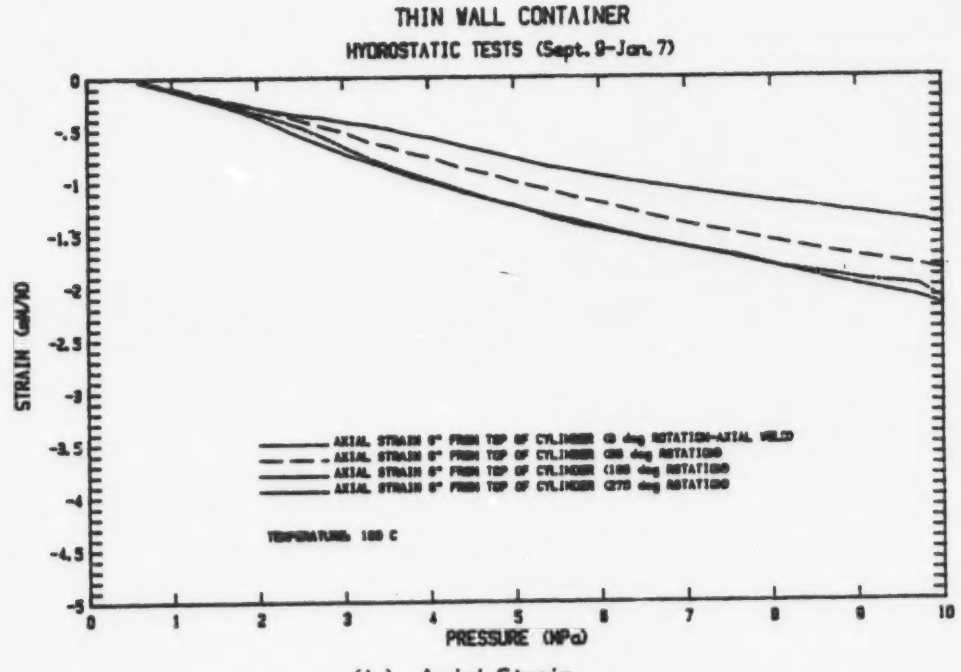

(b) Axial Strain

PLOT 3

STRAIN IN CYLINDER BELOW TOP LID

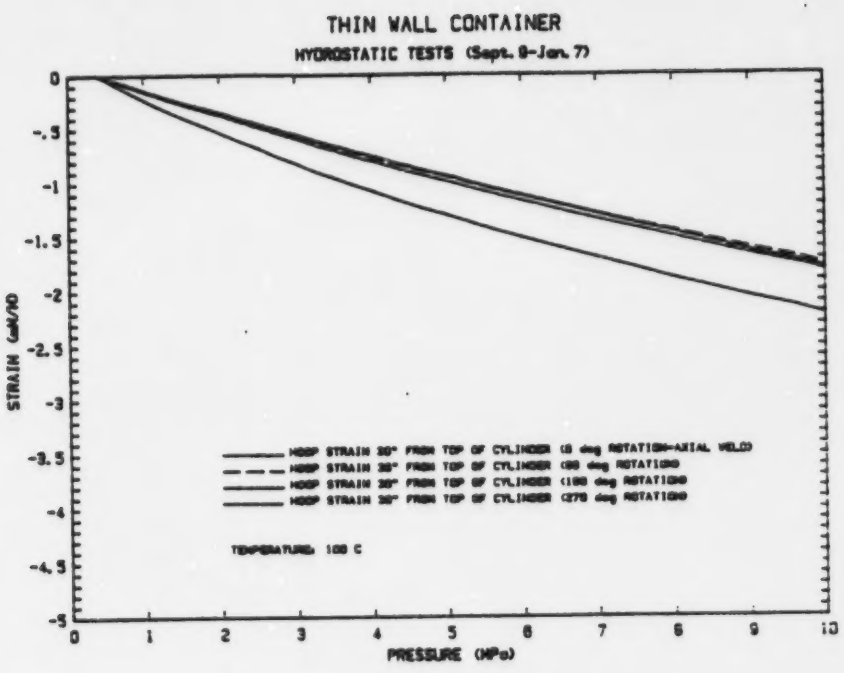

(a) Hoop Strain

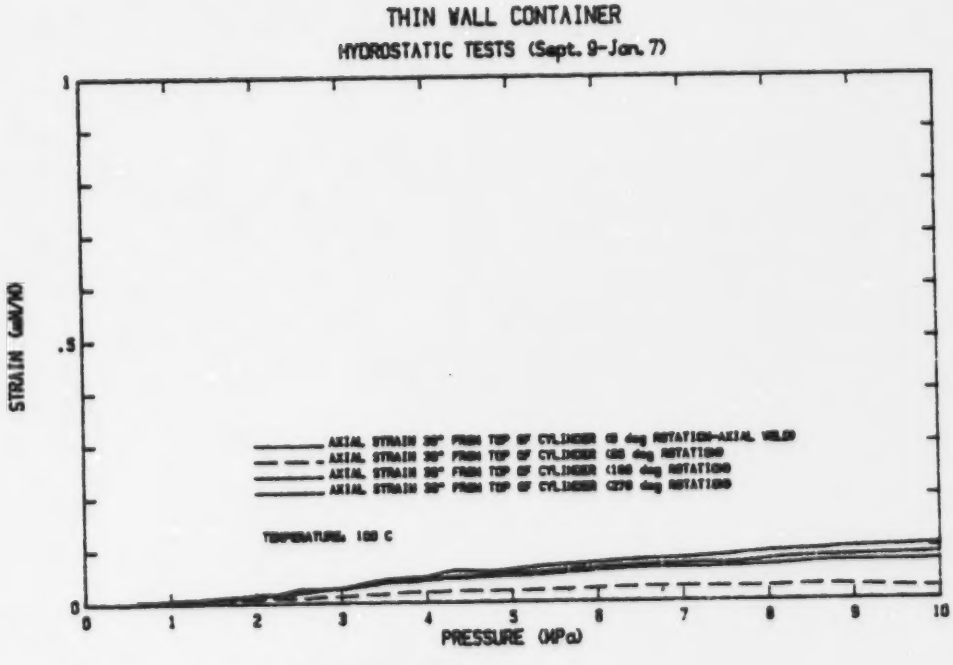

(b) Axial Strain

PLOT 4

STRAINS IN CYLINDRICAL SHELL
AWAY FROM DISCONTINUITIES

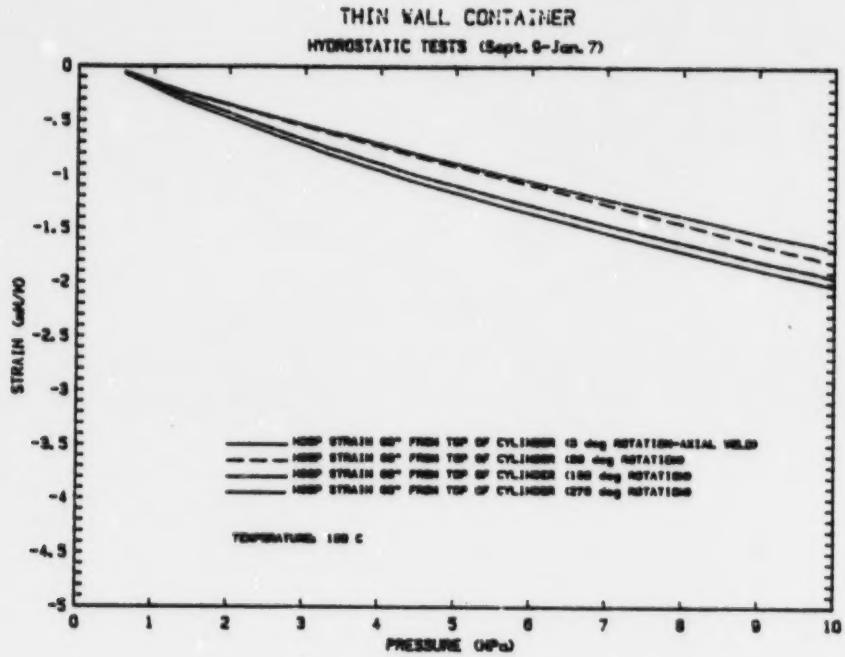

(a) Hoop Strain

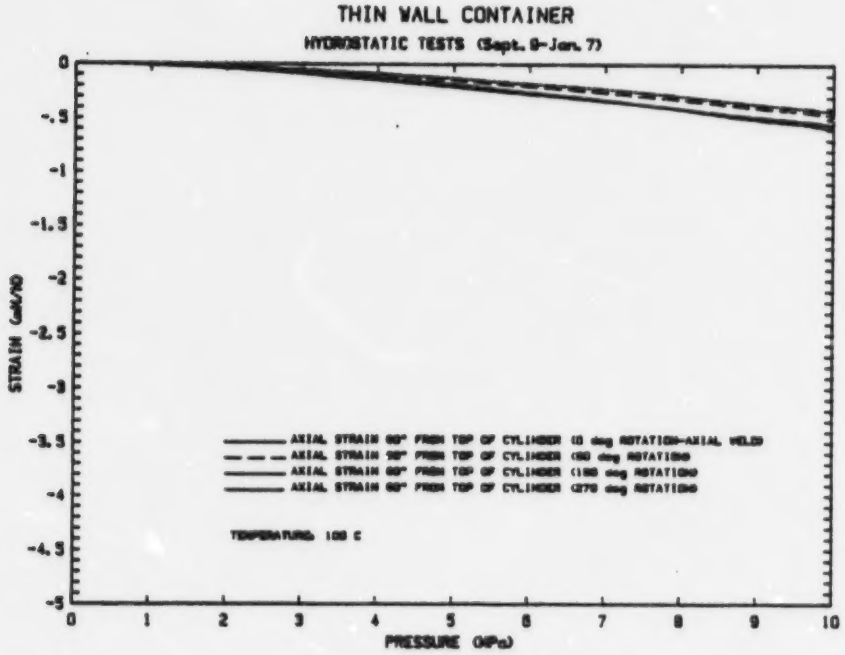

(b) Axial Strain

PLOT 5

STRAIN IN CYLINDER AT CIRCUMFERENTIAL WELD

166312 RD

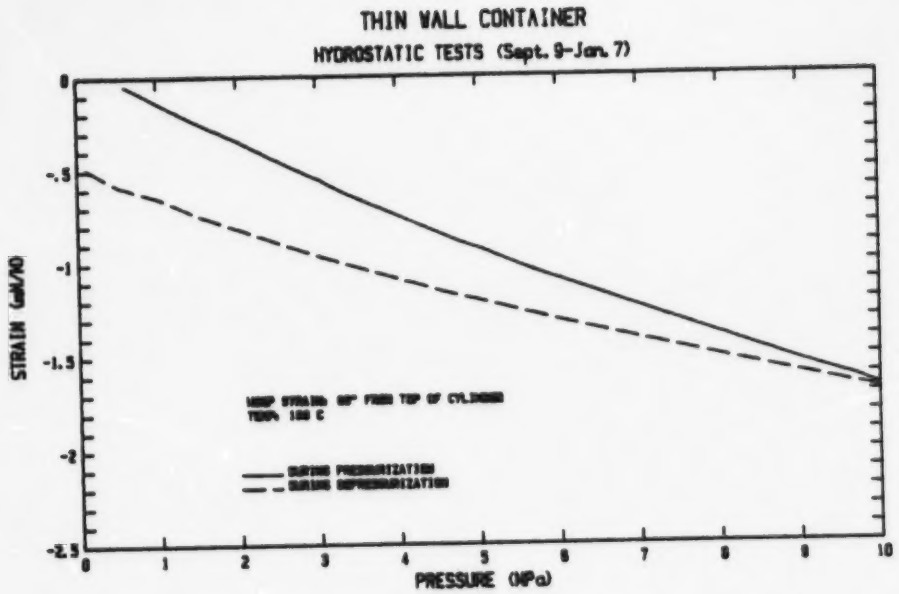

(a) Hoop Strain

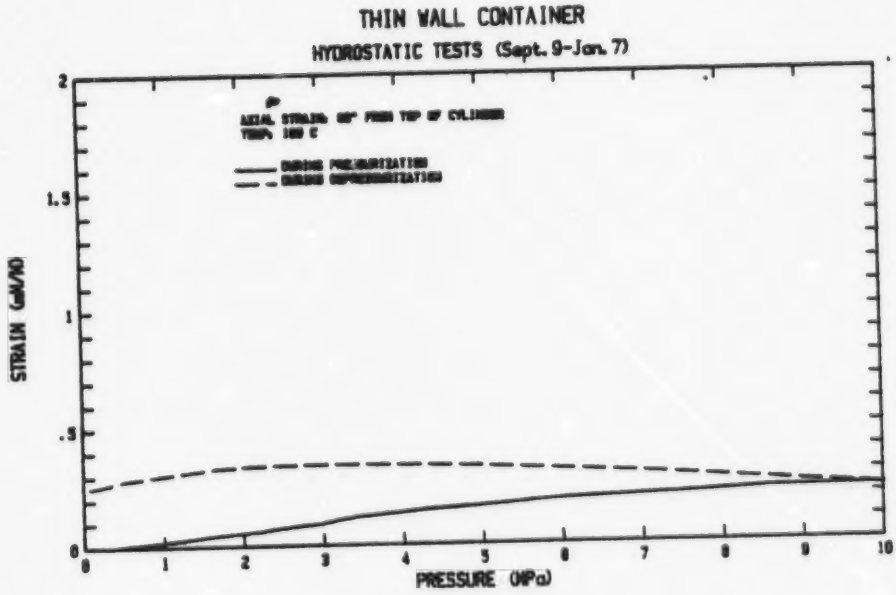

(b) Axial Strain

PLOT 6

STRAIN IN CYLINDER AT BOTTOM PLATE

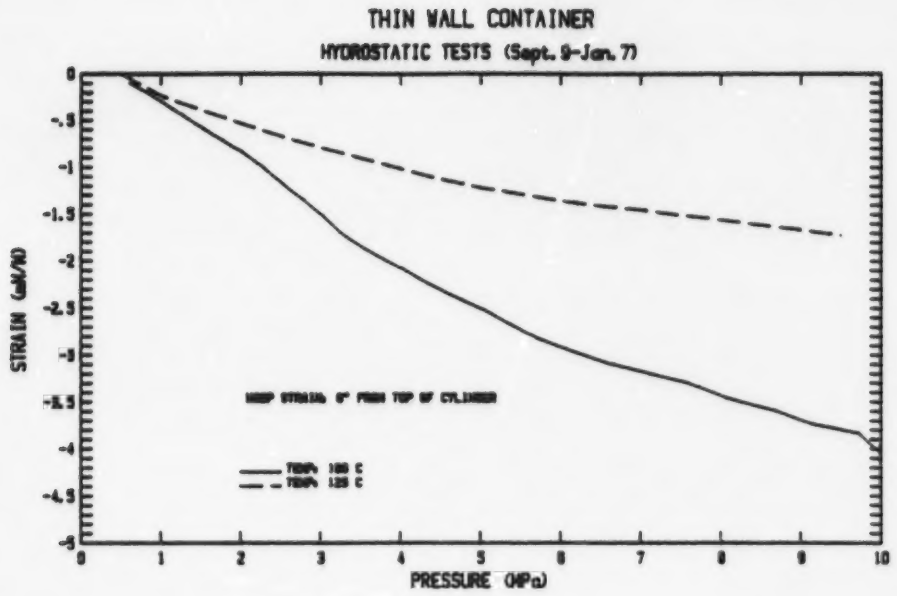

(a) 6" Below Top of Cylinder

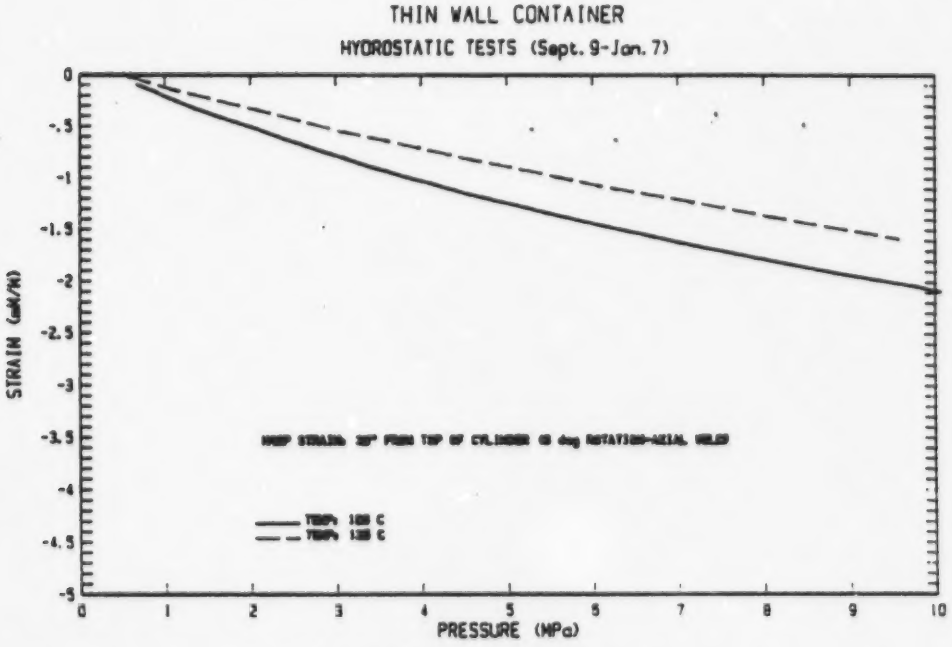

(b) 30" Below Top of Cylinder

PLOT 7A

STRAINS DURING 125° TEST - CYLINDRICAL SHELL

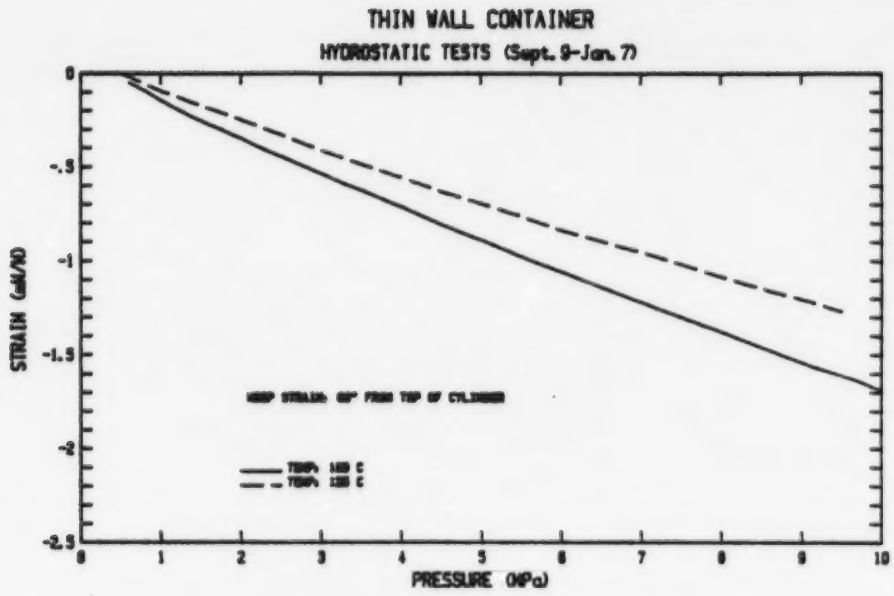

(c) 60" Below Top of Cylinder

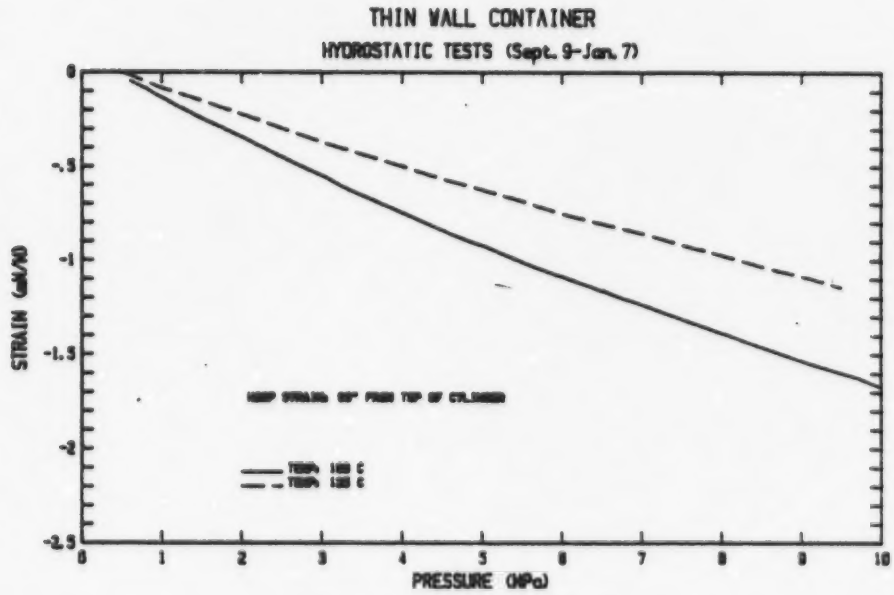

(d) Above Bottom Lid

PLOT 7B

STRAINS DURING 125°C TEST - CYLINDRICAL SHELL

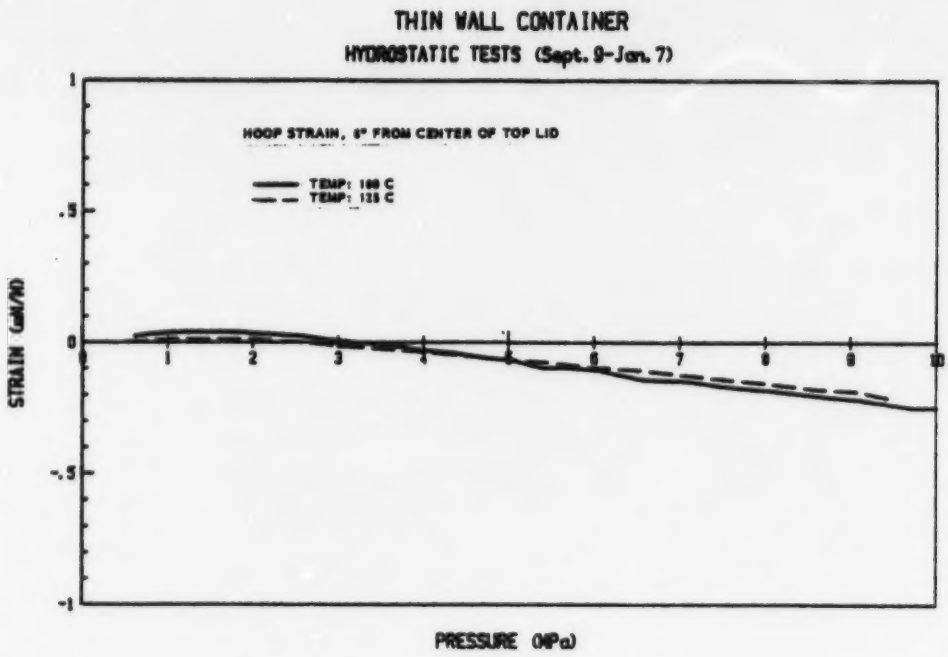

(a)

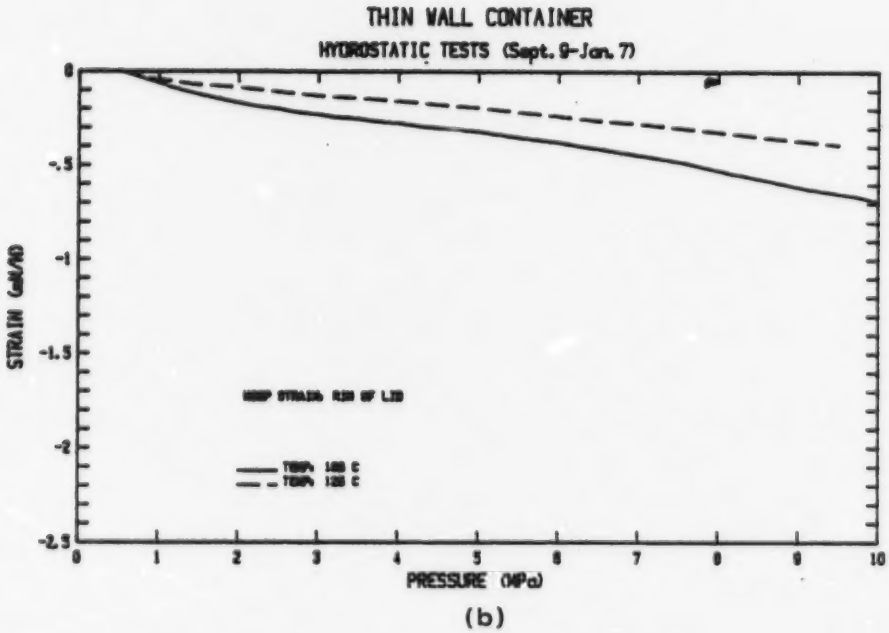

(b)

PLOT 8

STRAINS DURING 125°C TEST - TOP PLATE

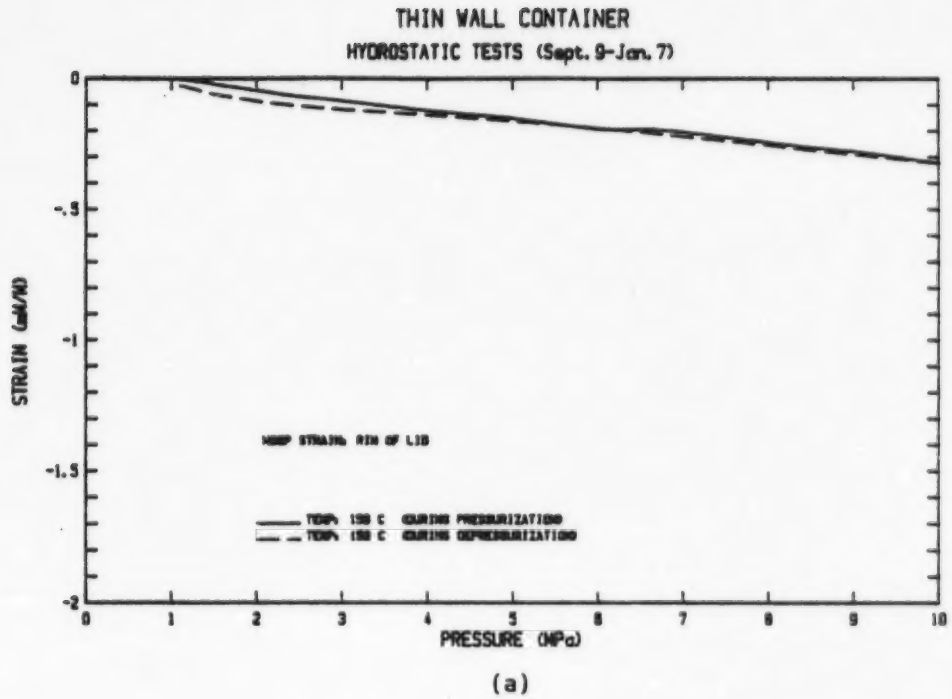

(a)

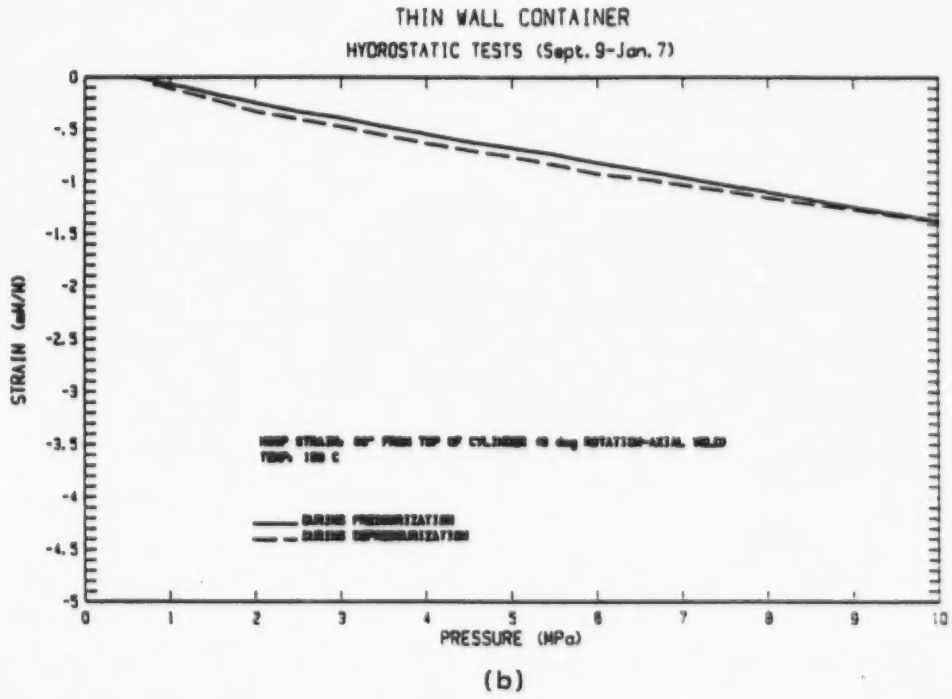

(b)

PLOT 9

PRESSURE CYCLE DURING 150°C TEST

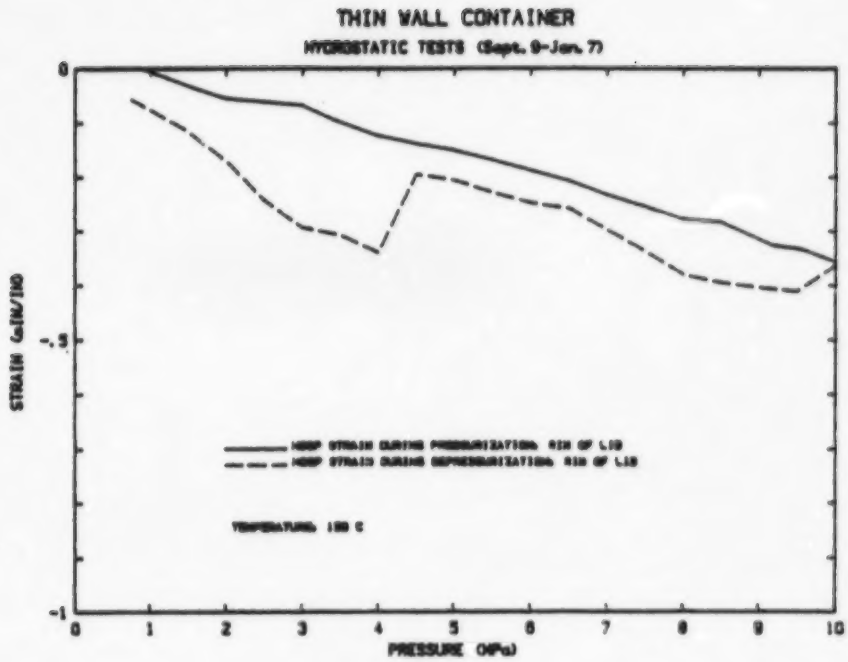

PLOT 10

LOCAL INSTABILITY

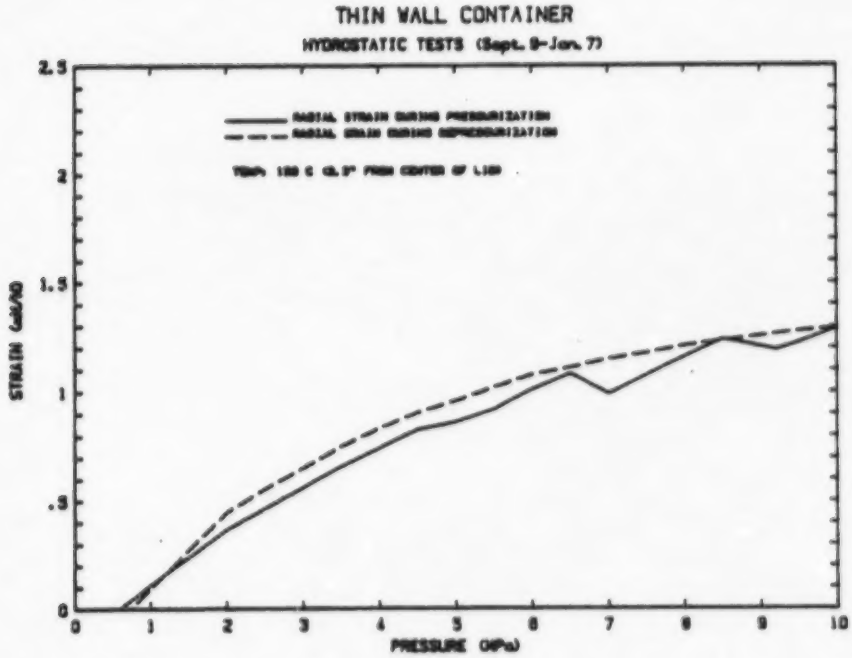

PLOT 11

EXPECTED VARIATIONS IN STRAIN GAUGE READINGS

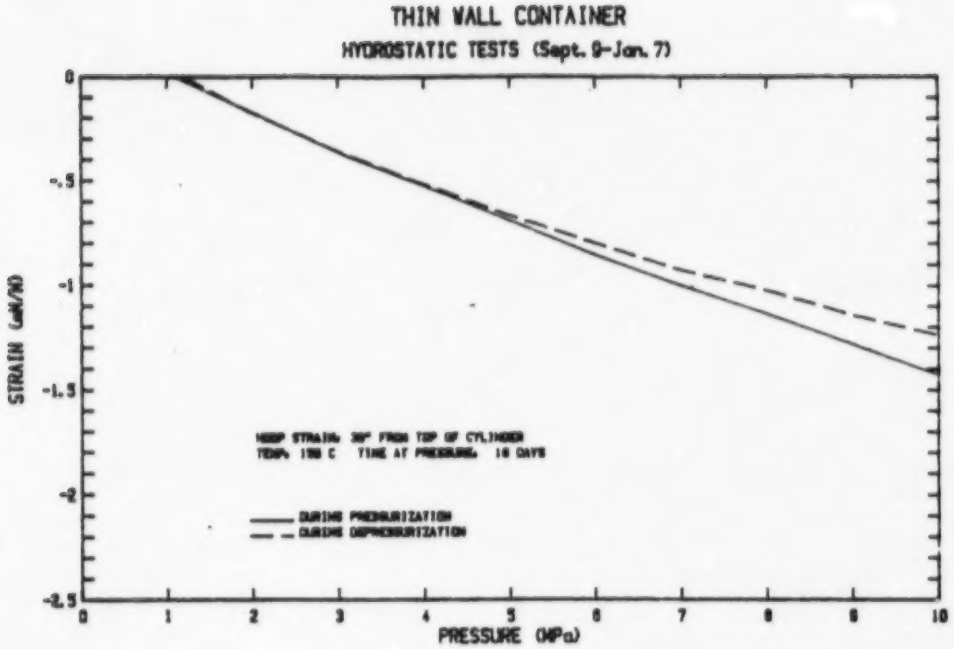

(a) Pressurization and Depressurization

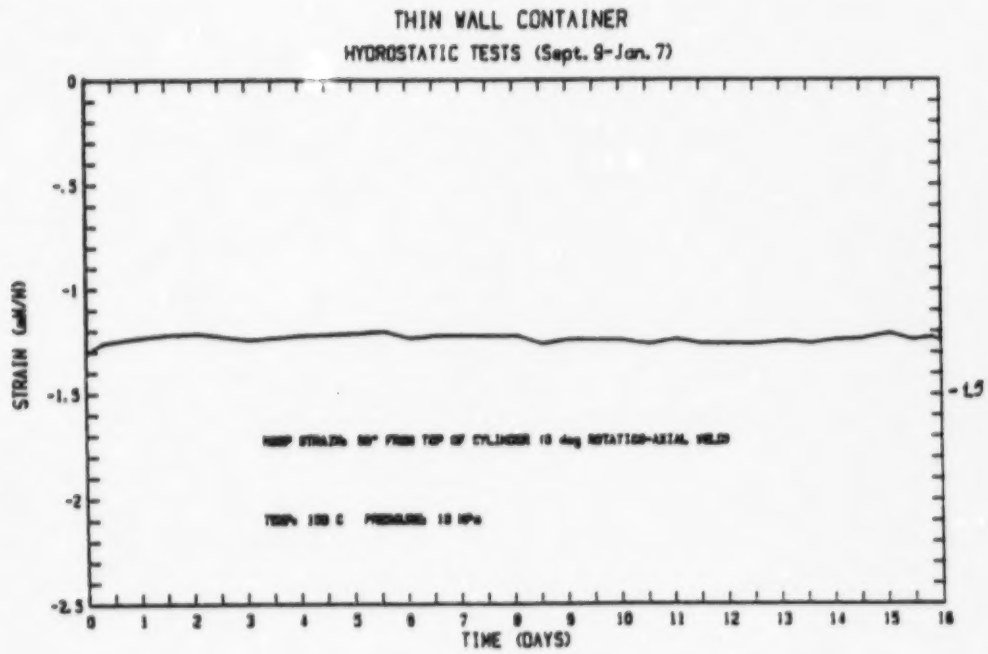

(b) Steady State Test

PLOT 12

LONG TERM TEST RESULTS AWAY FROM DISCONTINUITIES

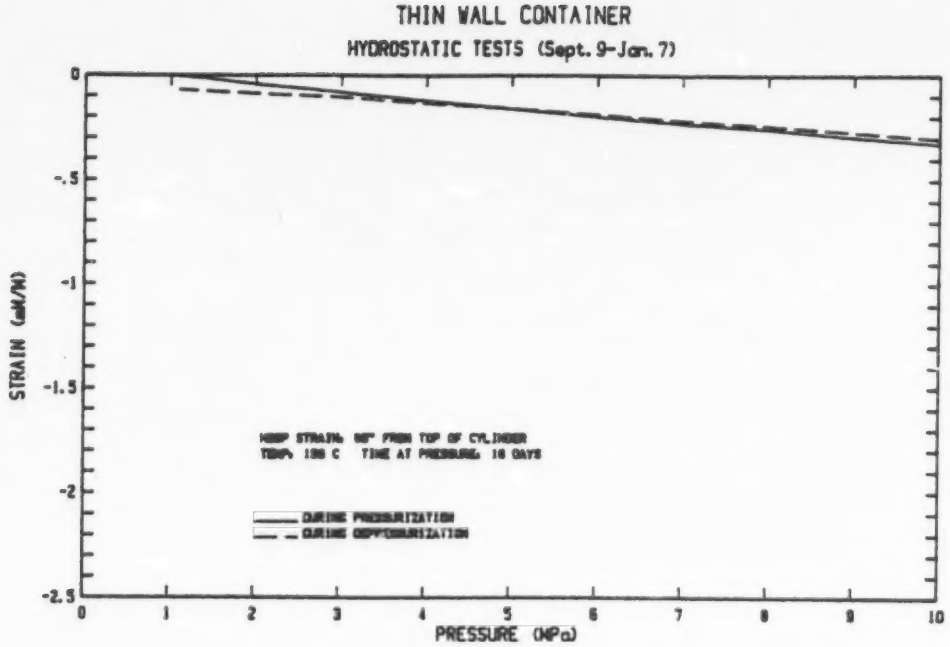

(a) Pressurization and Depressurization

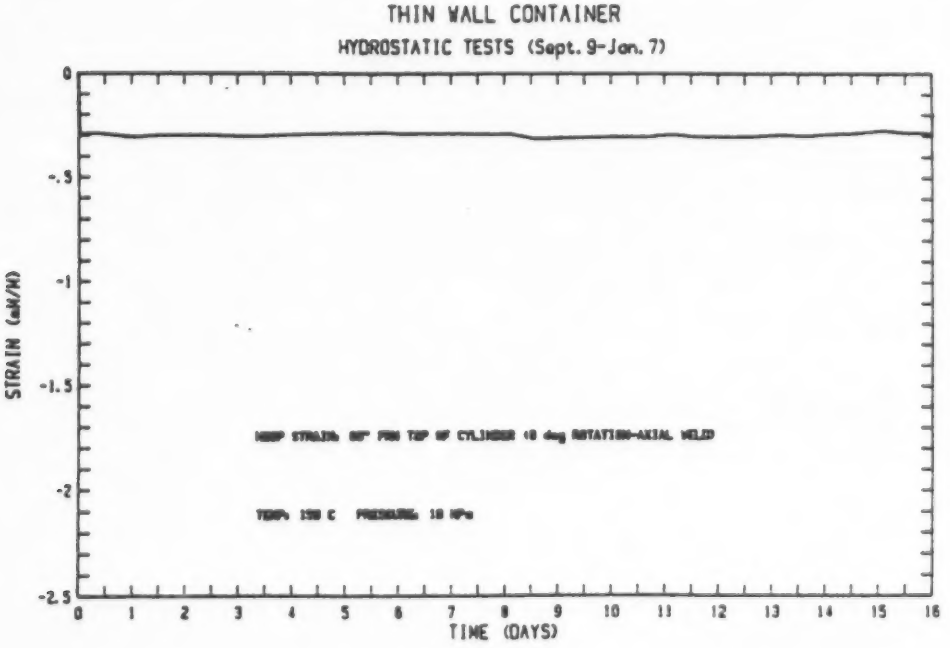

(b) Steady State Test

PLOT 13

LONG TERM TEST RESULTS NEAR BOTTOM LID

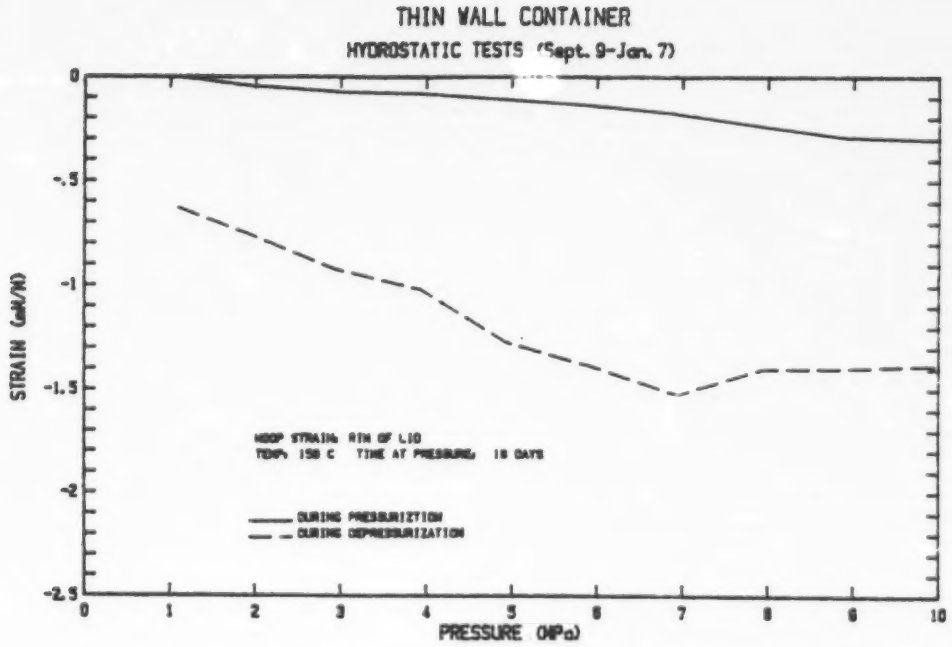

(a) Pressurization and Depressurization

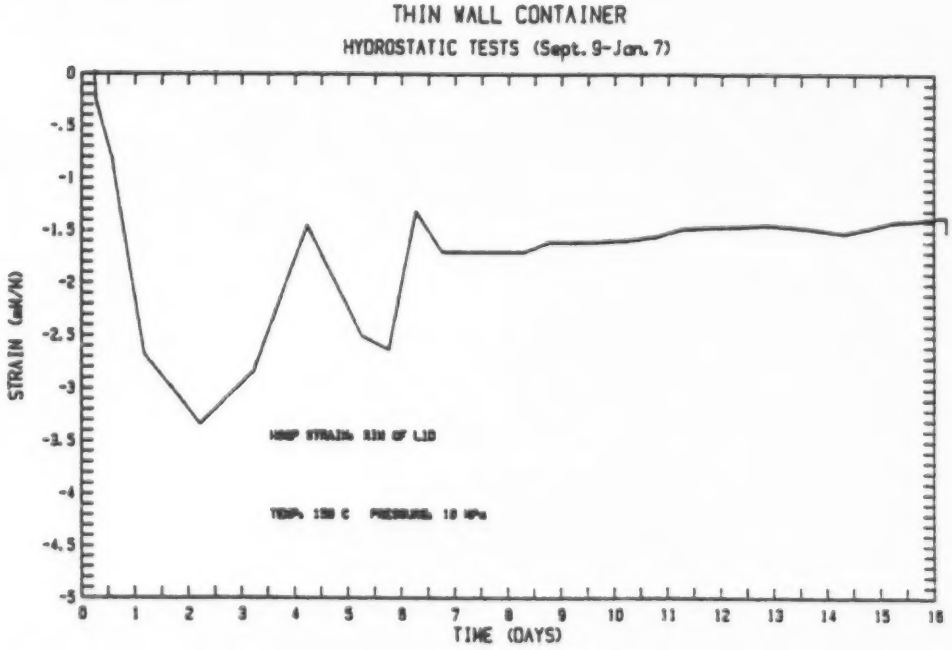

(b) Steady State Test

PLOT 14

LONG TERM TEST RESULTS - RIM OF TOP LID

166321 RD

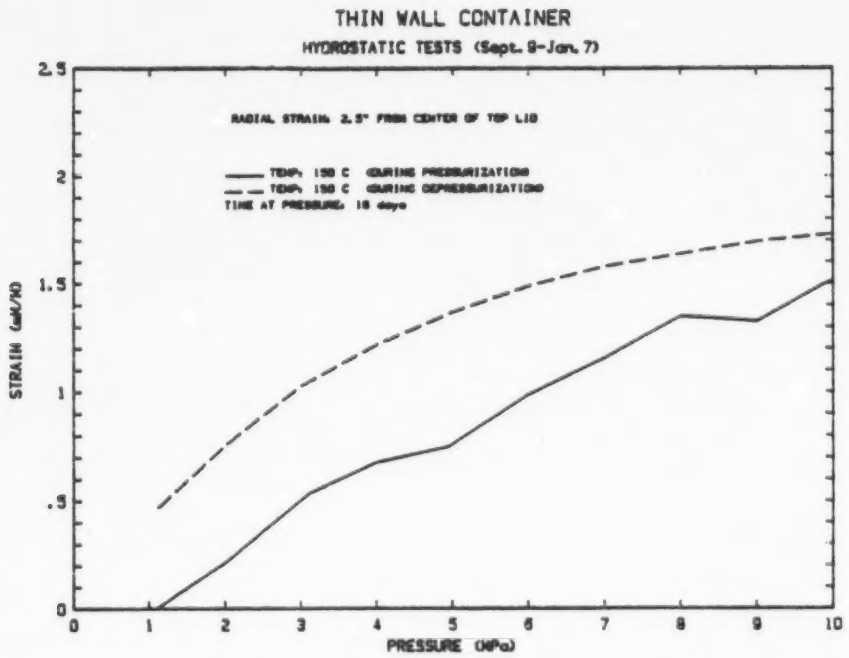

(a) Pressurization and Depressurization

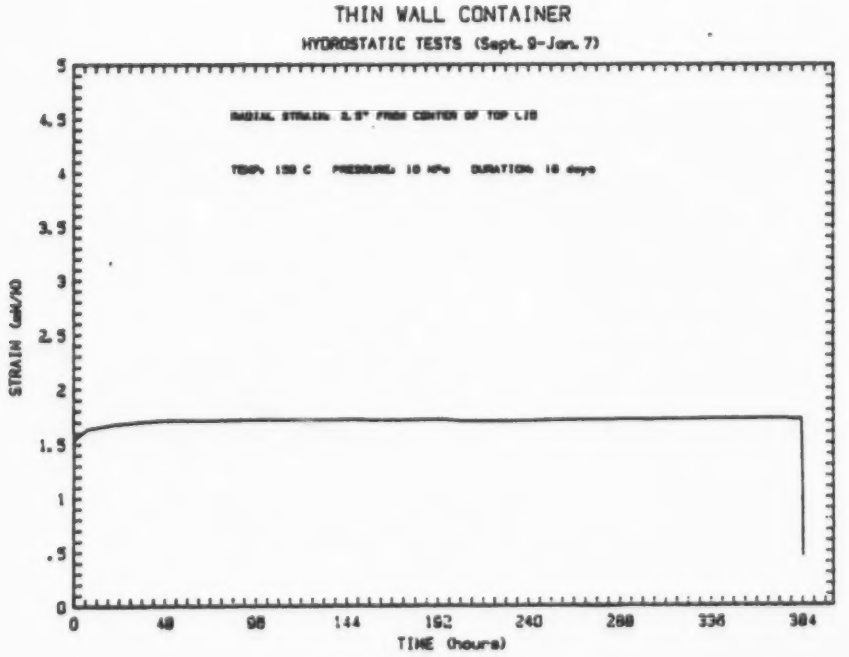

(b) Steady State Test

PLOT 15

LONG TERM TEST RESULTS -
NEAR CENTRE OF TOP LID

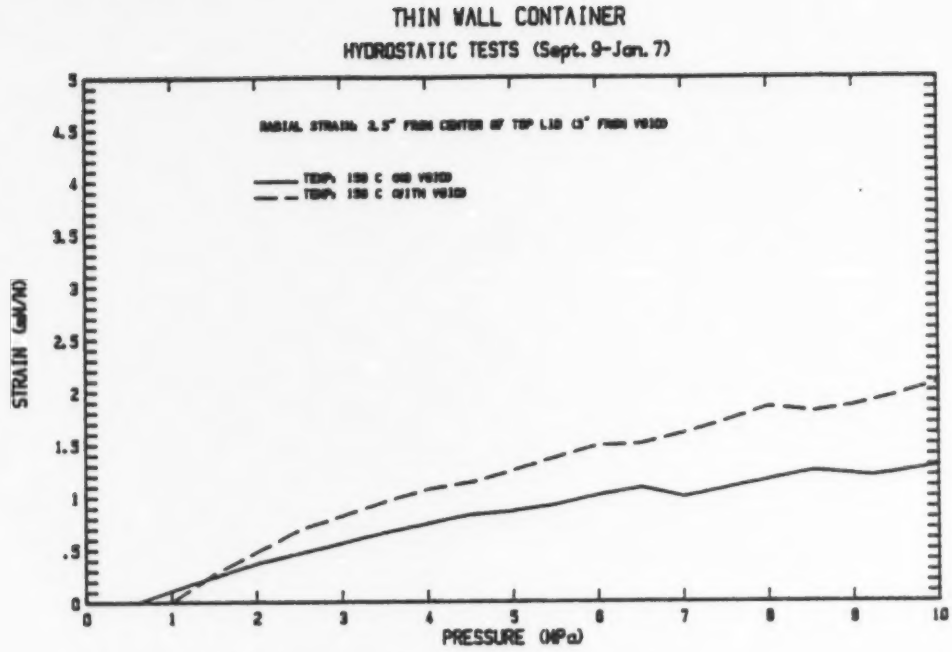

PLOT 16

STRAIN AT THE CENTRE VOID

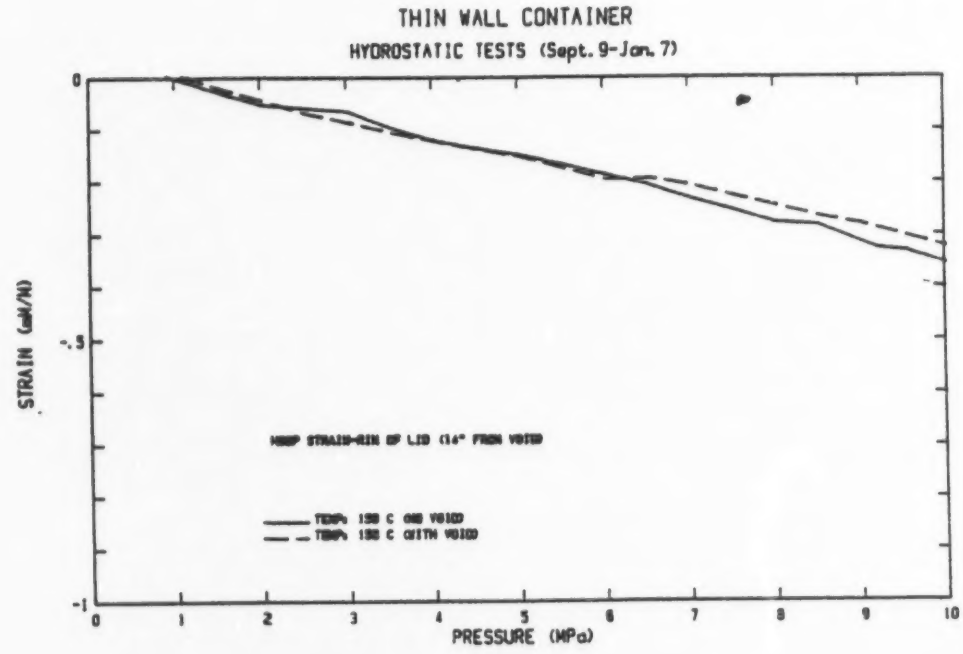

PLOT 17

STRAIN AWAY FROM CENTRE VOID

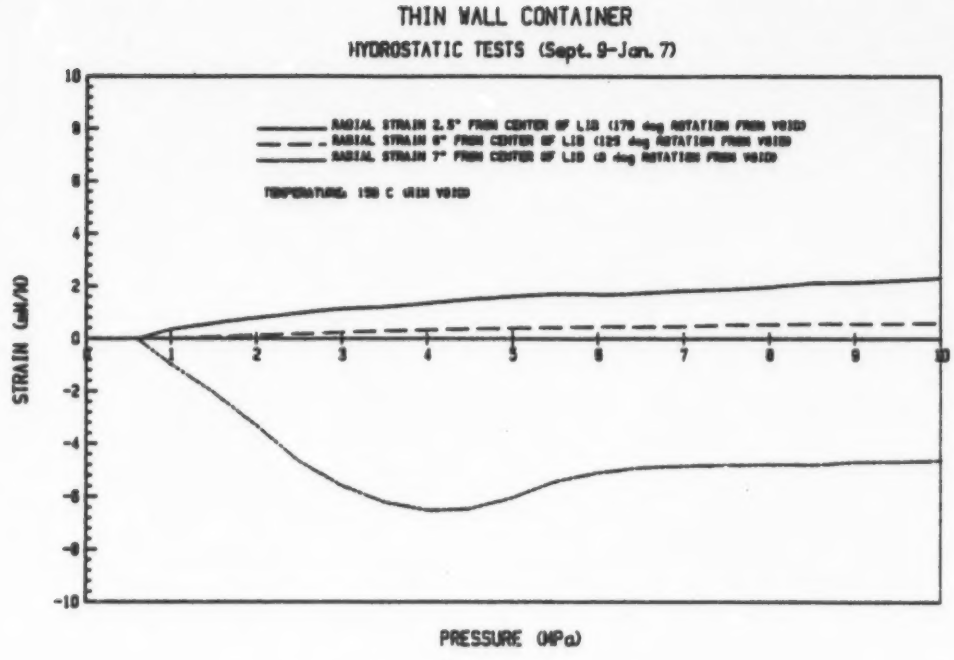

(a) Strain Pattern in Top Lid

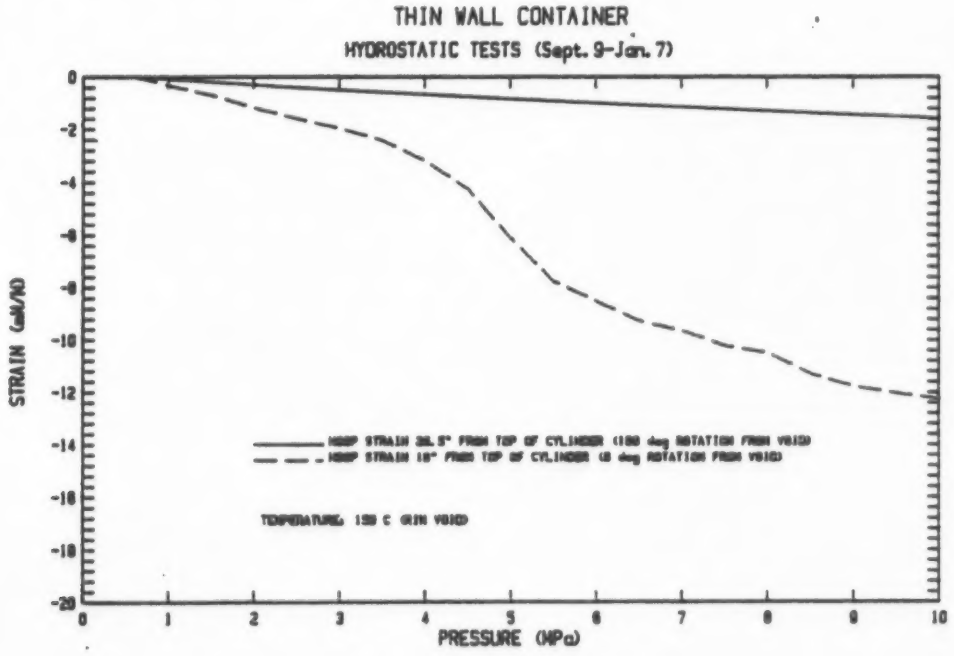

(b) Strain Patterns in Cylindrical Shell

PLOT 18

STRAIN AS A FUNCTION OF DISTANCE FROM RIM VOID

166324 RD

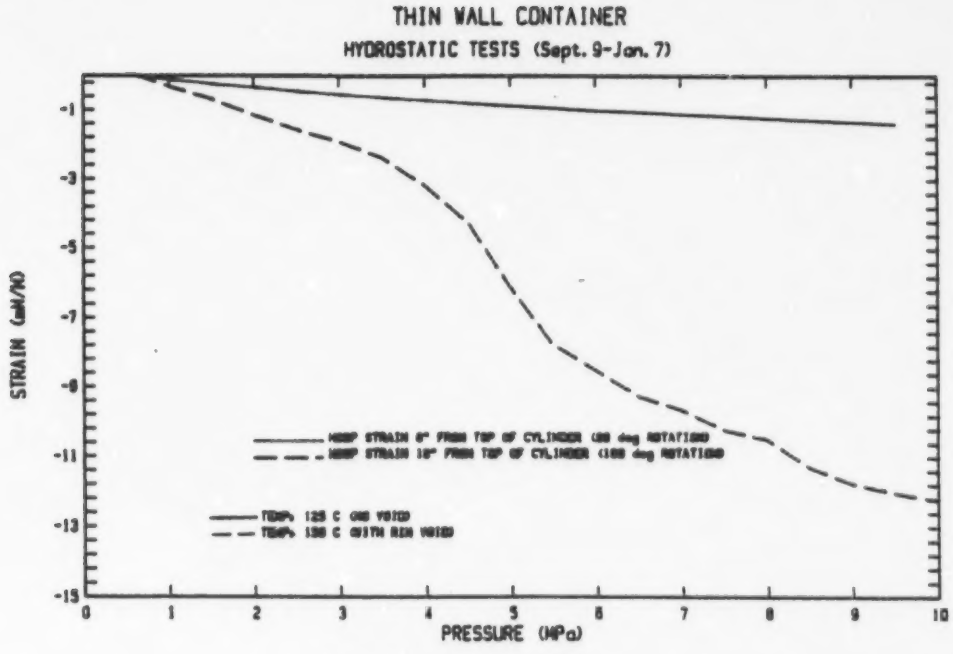

(a) Near Rim Void

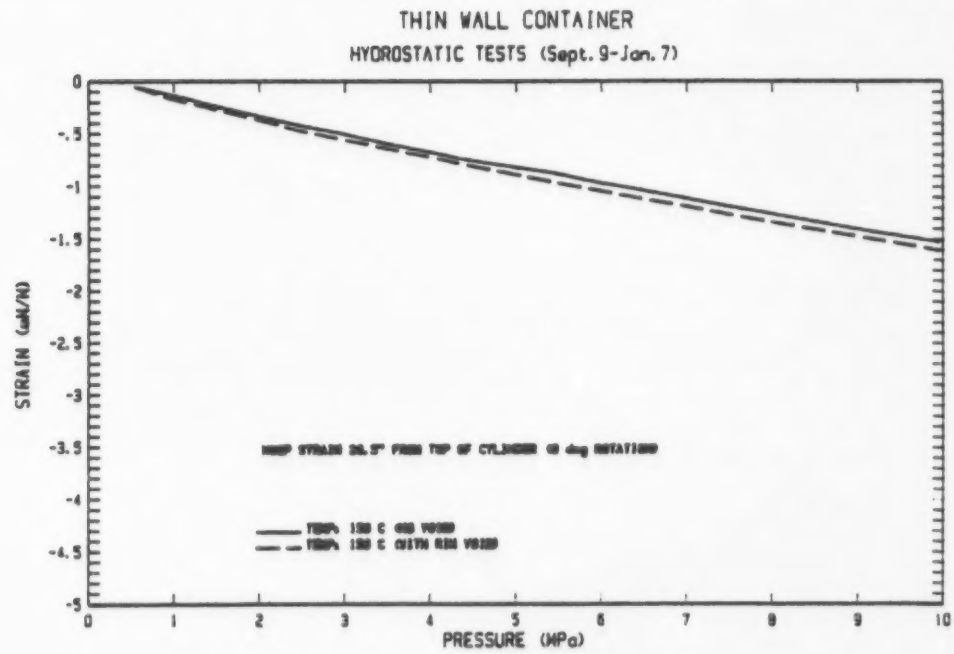

(b) Away From Rim Void

PLOT 19

COMPARISON OF STRAINS WITH AND WITHOUT RIM VOID

APPENDIX D

SEAL FAILURE

The top flange of the pressure vessel discussed in Subsection 6.1 can be opened and closed quickly. The flange is sealed with an O-ring type gasket. This gasket can be easily damaged and should be replaced frequently during a multi-stage test program, as illustrated by the accident described here.

The same O-ring was used during the preliminary tests, the first-stage test and the second-stage test. However, when the pressure inside the vessel reached about 9.8 MPa, the O-ring was extruded from the flange. The O-ring was torn. Several pieces of the O-ring were found during the post-failure clean-up, see Figure D-1. In a few seconds, following the gasket failure, the room filled with steam and all personnel had to be evacuated from the building. Test monitoring equipment tracked the conditions inside the vessel following the ring failure. The data seems to be scattered due to the flashing steam. The results are shown in Figure D-2. Personnel returned to the building two hours after the gasket failure. The room was covered with water and steam (see Figure D-3), although a large opening in the roof was cleared.

The torn gasket was carefully examined after the vessel was opened (see Figure D-4).

The test program was delayed due to the damage to the vessel, as a result of the accident. Loss of insulation on the upper head is shown in Figure D-5. An attempt to open the vessel fast, resulted in a bent stop system, shown in Figure D-6.

A new gasket was used for each remaining stage of the test program. This was the only gasket failure during this test program.

The test monitoring equipment was turned off several minutes after the seal failure. After a 24-hour drying period, the equipment was shown to operate properly.

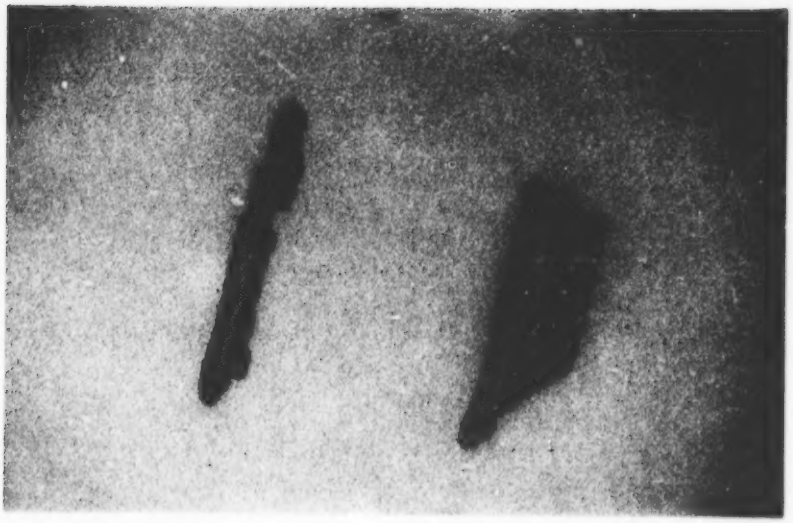

FIGURE D-1
TORN-OFF PIECES OF THE SEAL

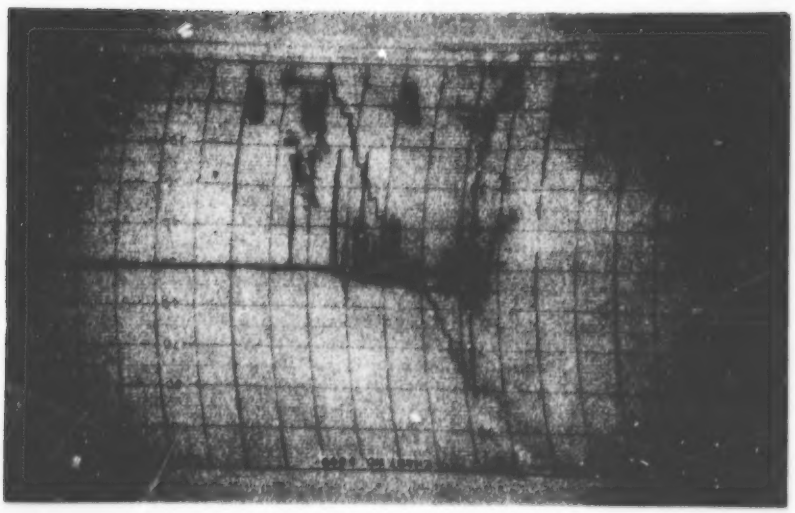

FIGURE D-2
PRINTOUT OF PRESSURE, TEMPERATURE AND
WATER LEVEL AT SEAL FAILURE

(a) Test Facility Two Hours After Seal Failure

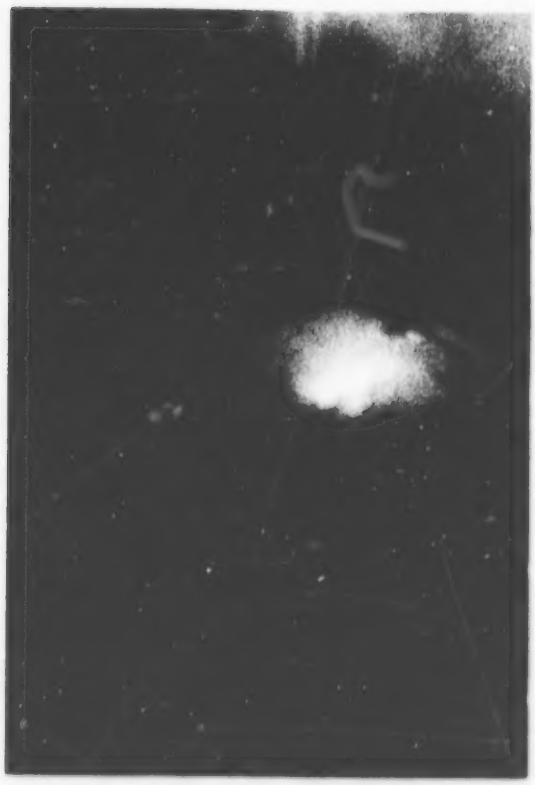

(b) Three Hours After Seal Failure

FIGURE D-3

(a) Top Part

(b) Bottom Part

FIGURE D-4
TORN GASKET

FIGURE D-5
INSULATION DAMAGE

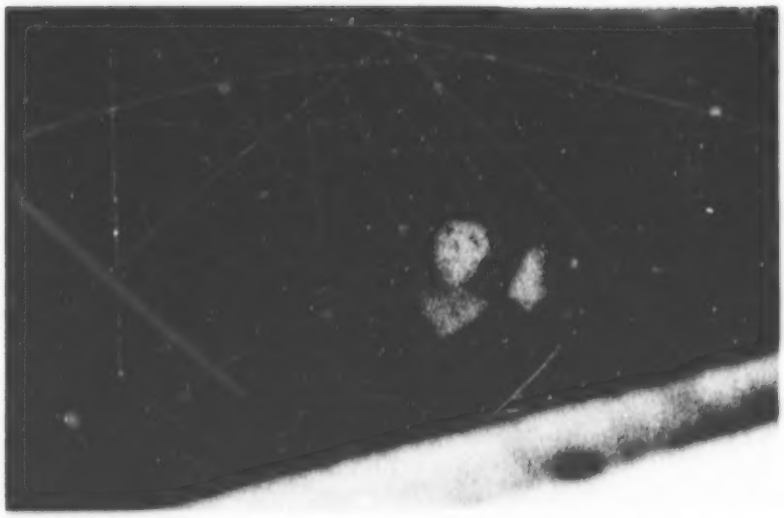

FIGURE D-6
DAMAGED STOP

APPENDIX E

PARTICULATE STIFFNESS CONSIDERATION

TABLE OF CONTENTS

Page

E-1 Strength of Particulates

E-2 Stiffness of Particulate

E-3 Stiffness of Cylindrical Shell

E-4 Stability of Cylinder

E-5 Flat Plates

E-6 Axial Strain Consideration

E-7 Discussion

E-1 Strength of Particulates

Unconfined granular materials have no strength - their shear modulus and modulus of elasticity are zero. However, when compressive forces are applied, friction forms between grains of particulate, giving an impression of shear strength. For example, a 40° sloped pyramid of particulate can support large forces (see Figure E-1) by transfering the forces to the solid base through friction (apparent shear). The friction forces give particulate large strength, which is a function of load.

By measuring shear forces in our test program, we have evaluated the shear modulus of elasticity (G) and Poisson's ratio (υ) for various granular materials. Since most stress analysis computer codes do not allow Young's modulus (E) to be equal to zero, and for easier comparison with solids (metals), we have assumed an artificial value for the modulus as follows:

$$E = 2G(1+\upsilon)$$

Although this assumption introduces a significant error, it is useful in establishing a general tendency in stresses and deformations, as shown in Section 6. We must also realize that this modulus varies with external pressure for granular materials, as shown in Figure F-3.

E-2 Stiffness of Particulate

The stiffness of various particulates was evaluated in a set of tests preceding the construction of the prototype/3/. The stiffness of particulates was relatively low if compared with solid titanium or steel. Table E-1 shows the Young's Modulus of elasticity of particulate to vary from 0.1% to 0.65% of the modulus of titanium. Glass beads have the least stiffness.

We assumed that our particulate consists of perfect spheres all having the same diameter, for analytical derivation of stiffness of particulate. Furthermore, we assumed that the spheres are organized in fase center cubic orientation, for largest stiffness. Based on the Hertz contact stress theory, we have shown the "effective Young's Modulus" of particulate to be:

$$E_p = 1.044 \sqrt[3]{pE^2}$$

or

$$E_p/E \approx \sqrt[3]{(p/E)}$$

where E_p - modulus of elasticity of particulate
E - modulus of elasticity of equivalent solid material
p - external pressure.

Sample calculations of this equation for steel, titanium and glass are shown in Figure E-3. From this equation, ratio of moduli for different particulates is:

$$E_{p_1}/E_{p_2} = (E_1/E_2)^{0.667}$$

This equation is plotted in Figure E-2. It should be noted that increase in modulus of solid material results in a smaller increase in modulus of particulate.

E-3 Stiffness of Cylindrical Shell

Titanium is 150 to 1200 times stiffer than granular materials tested. However, if we define stiffness of cylindrical shell as a ratio of external pressure to radial strain

$$E_c = p/(\Delta r/r)$$

than our particulate have a more compatible stiffness with the cylinder.

For a long cylindrical shell:

$$E_c = (t/r)E$$

where: t - wall thickness
r - radius of cylinder.

For our titanium container:

$$E_c = 1\ 550\ \text{MPa}$$

This calculation does not account for any instability effects because particulate prevents large buckling, as we saw during the hydrostatic tests.

E-4 Stability of Cylinder

It was shown above that the titanium shell is about 15 times stiffer than the particulate. In Part 5, it was shown that the particulate in bulk is actually stiffer than the cylindrical shell, because of the buckling instability of the cylinder. A long cylinder is expected to become unstable under an external pressure:

$$p = 0.25[E/(1-\upsilon^2](t/r)^3$$

$$= 0.18 \text{ MPa.}$$

This pressure was attained during an initial sealing of the vessel and before any strain measurements could be taken. The preliminary tests, discussed in Section 6.2 were conducted to demonstrate the stability of our particulate supported container.

E-5 Flat Plates

The top and bottom closures of the container are in form of flat plates. Deformation of flat plates under pressure is high. Again, we can calculate the siffness of the flat plates assuming that they are 50% built in:

$$E_p = p/(y/r) = 0.5[(15.7\ D/r^4) + (64\ D/r^4)]$$

$$= 1.2 \text{ MPa.}$$

The cylindrical shell and the flat plates have little stiffness and rely fully on particulate for support.

E-6 Axial Strain Consideration

If we would look at the titanium shell as a thin-wall container under pressure, the axial strain should be equal to one half of the hoop strain, as measured by the strain gauges, near the top plate, during the hydrostatic test program. This axial strain is the result of the external pressure acting on the end plates. In the particulate filled container, this axial pressure is supported by the particulate, after significant deformation of top plates took place. The axial strain is only seen at the top discontinuity because the gauges are mounted above the level of the settled particulate.

E-7 Discussion

Although the tested particulates are much softer than solid metals, their stiffness is comparable to that of the cylindrical shell and much higher than flat plates. In the hydrostatic test program, the particulate successfully performed three functions:

a) It maintained the end plates flat and prevented their failure.

b) It prevented buckling of cylindrical shell.

c) Stiffness of the cylindrical shell could contribute to the overall container performance because it was geometrically stable. Stiffness of cylindrical shell is shown by Line 10 in Figure E-3.

TABLE E-I
STRENGTH OF PARTICULATES

No.	Particulate or Solid Material	Test Pressure MPa	ν	E_p MPa	β MPa	E_p/E_t (1)
	PARTICULATES					
1	Wedron Sand	12.0	0.34	193	200	0.0020
2	Glass Beads 0.6-0.9	12.0	0.45	103	365	0.0010
3	Glass Beads 1.0-1.2	12.0	0.40	159	269	0.0016
4	Glass Beads 1.4-1.68	12.0	0.40	152	269	0.0015
5	Steel Shots	12.0	0.32	648	607	0.0065
6	Bauxite	12.0	0.33	43	83	0.0008
7	Analyzed Particulate	--	0.40	250	417	--
	PARTICULATE WITH BUNDLE					
8	Wedron Sand	9.7	0.26	1,662	1,151	0.0166
9	Glass Beads 0.6-0.9	9.7	0.18	2,337	1,220	0.0234
10	Glass Beads 1.0-1.2	9.7	0.34	1,041	1,055	0.0104
	SOLID MATERIALS					
11	Steel	--	0.29	200,000	160,000	2.00
12	Titanium	--	0.34	100,000	110,000	1.00
13	Glass(3)	--	0.20	69,000	38,000	0.69
14	Quartzite	--	0.14	82,700	38,300	0.83
	PARTICULATE - LAMBE AND WHITMAN DATA (2)					
15	Sand	--	0.2-0.5	103	--	0.001

(1) E_t = 100,000 MPa - Young's modulus of titanium

(2) See Reference 1

(3) The shown values are for illustration only as they vary widely with compostion and treatment.

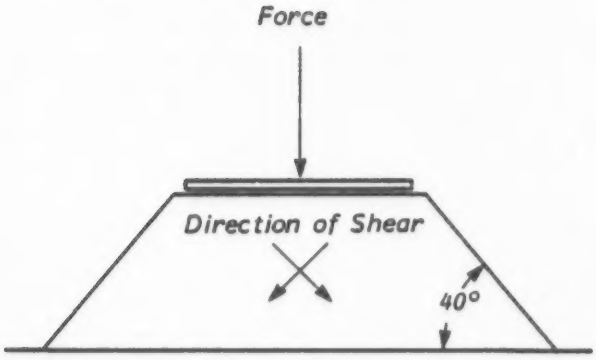

FIGURE E-1
SHEAR STRENGTH OF PARTICULATE

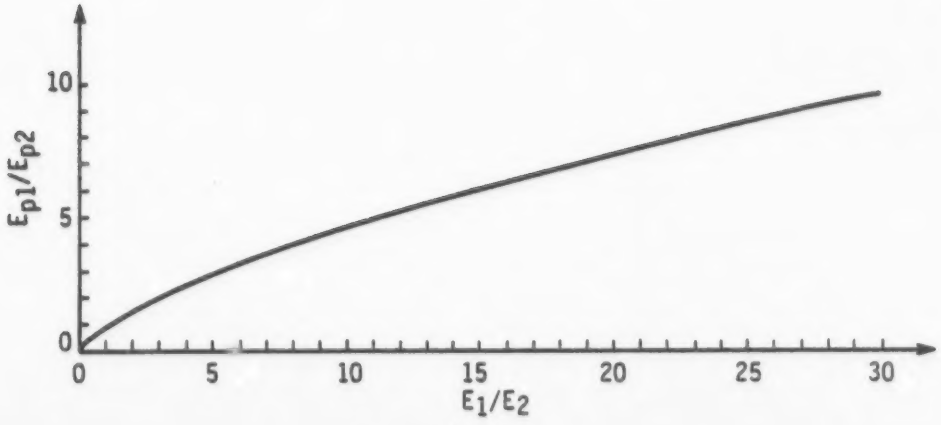

FIGURE E-2
COMPARISON OF MODULI OF ELASTICITY

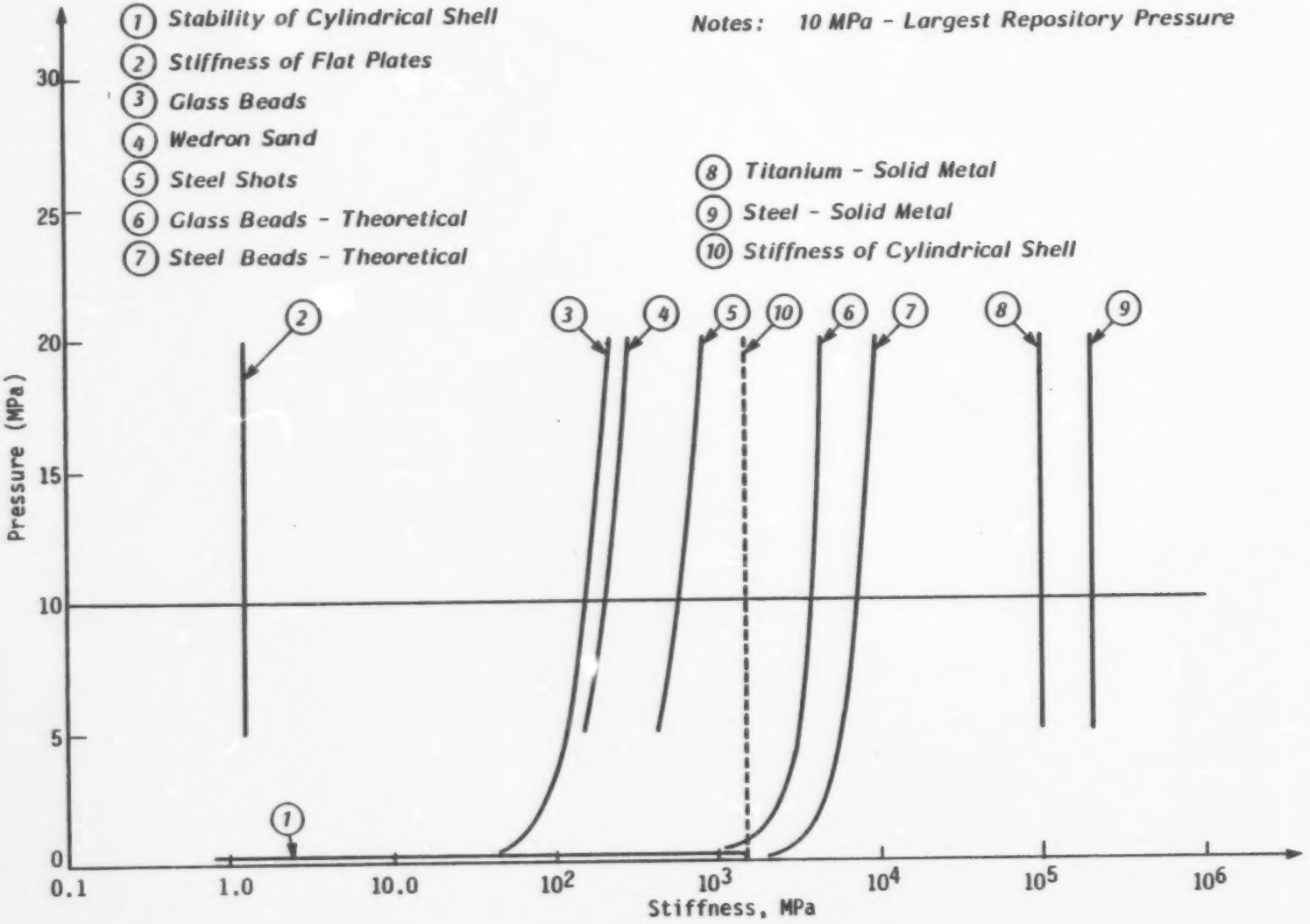

FIGURE E-3
STIFFNESS OF VARIOUS MATERIALS